IJE TRANSACTIONS C: Aspects Vol. 26, No. 12, (December 2013) 1445-1460

International Journal of Engineering

Journal Homepage: www.ije.ir

Three-dimensional Magneto-thermo-elastic Analysis of Functionally Graded Truncated Conical Shells

A. Mehditabar, R. Akbari Alashti*, M. H. Pashaei

Mechanical Engineering Department, Babol University of Technology, Babol, Iran

PAPER INFO

Paper history:
Received 17 April 2013
Received in revised form 18 June 2013
Accepted 20 June 2013

Keywords:
Magneto-thermo-elastic
Functionally Graded Material
Truncated Conical Shell

ABSTRACT

This work deals with the three-dimensional magneto-thermo-elastic problem of a functionally graded truncated conical shell under non-uniform internal pressure subjected to magnetic and thermal fields. The material properties are assumed to obey the power law form that depends on the thickness coordinate of the shell. The formulation of the problem begins with the derivation of fundamental relations of thermo-elasticity in the conical coordinate system. Subsequently, the differential quadrature method (DQM) is employed to discretize the resulting differential equations and transform them into a system of algebraic equations. Numerical results are presented to illustrated effects of non-homogeneity properties of material and thermal loads on the distributions of displacement, stress, temperature and induced magnetic fields. Finite element method is used to validate the results of DQM for a functionally graded truncated conical shell which shows excellent agreement.

doi: *10.5829/idosi.ije.2013.26.12c.05*

NOMENCLATURE

K	Coefficient of heat conductivity	T_i	Inner surface temperature of the cone
σ_{ij}	Components of stress tensor	T_o	Outer surface temperature of the cone
α	Coefficient of thermal expansion	λ, G	Lame's constants
$\vec{U}$	Displacement vector	L	Length of the generator of the cone
u, v, w	Displacement components	f_l	Lorentz's force
L_1	Distance between the origin and the top surface of the cone	$\vec{H}$	Magnetic field vector
E_0	Elastic constant	μ	Magnetic permeability
$\vec{J}$	Electric current density vector	N, M, P	Number of grid points along the thickness, circumferential and generator, respectively
$\vec{h}$	Induced magnetic field vector	υ	Poisson's ratio
R_1	Inner radius of the cone at its small end	γ	Semi-vertex of the conical shell
R_2	Inner radius of the cone at its large end	h_{sh}	Thickness of the shell m
n	Inhomogenity constant	$A^{(n)}, B^{(n)}, C^{(n)}$	Weighting coefficients of the n^{th} derivative along the thickness, generator and circumference, respectively

1. INTRODUCTION

Nowadays, the magneto-thermo-elasticity theory that deals with the interaction between different physical fields has been the subject of high level researches. It is found that a conducting truncated conical shell under the effect of magneto-thermo-elastic field, experiences combination of different kinds of loads such as the Lorentz force exerted by the applied primary magnetic field, thermal load and also the internal pressure, simultaneously. The aim of the magneto-thermo-elastic stress analysis is usually to determine whether a

*Corresponding Author Email: raalashti@nit.ac.ir(R. Akbari Alashti)

structure under a prescribed loading behaves as desired or not. Hence, determining the distribution of stress field is the top priority of an engineering design [1].

During the last decade, tremendous research efforts have been devoted to optimize materials performances and promote their load bearing capabilities. In order to accomplish this task, a revolutionary design paradigm of the material technology is developed among which, the functionally graded material (FGM) is the most notable one. The basic concept behind FGMs is to engineer gradual variation or smooth change in the material properties in a structure. By virtue of gradients of material properties, an FGM posses some desirable characteristics such as high temperature resistance, thermal fatigue and impact performances [2].

Shadmehri et al. [3] proposed a semi-analytical approach to obtain the linear buckling response of conical composite shells under axial compression load. The principle of minimum total potential energy was used to obtain the governing equations and Ritz method was applied to solve them. Sofiyev et al. [4] studied the stability of three layered conical shell containing an FGM layer subjected to axial compressive load. The fundamental relations for stability and compatibility equations were transformed into a pair of time-dependent differential equations via Galerkin's method. Xu et al. [5] used the dynamic virtual work principal to derive non-linear equations of transverse motion of truncated conical shells. The Galerkin procedure was used to develop a system of equations for time functions which were solved by the harmonic balance method. Patel et al. [6] studied the thermo-elastic stability characteristics of cross-ply oval cylindrical/conical shells subjected to uniform temperature rise through non-linear static and finite element method. Zhang and Li [7] discussed the buckling behavior of functionally graded truncated conical shells subjected to normal impact loads and employed the Galerkin procedure and Runge-Kutta integration scheme to solve non-linear governing equations. Aghdam et al. [8] carried out bending analysis of moderately thick clamped FG conical panels subjected to uniform and non-uniform distributed loadings. The First Order Shear Deformation Theory (FSDT) was applied to derive the governing equations and Extended Kantorovich Method (EKM) was used to solve the equations. Wu et al. [9] presented the three-dimensional solution of laminated conical shells subjected to axisymmetric loadings using the method of perturbation. Petrovic [10] investigated stress analysis of a cylindrical pressure vessel loaded by axial and transverse forces on the free end of the nozzle applying the finite element method. Jabbari et al. [11] developed a general analysis of one-dimensional thermal stresses in a hollow thick cylinder made of functionally graded material, using the direct method to solve the governing equations. Eslami et al. [12] obtained a general solution for the one-dimensional steady state thermal and mechanical stresses in a hollow thick sphere made of functionally graded material. The analytical solution of heat conduction equation and the Navier equation were presented using the direct method. Paliwal and sinha [13] considered large deflection static analysis of shallow spherical shells on Winkler foundation, applying Bergler's and Modified Bergler's methods. Jane and Wu [14] studied thermo-elasticity problem in the curvilinear circular conical coordinate system. The hybrid Laplace transformation and finite difference were developed to obtain the solution of two dimensional axisymmetric coupled thermo-elastic equations. Chandrashekhara and bhimaraddi [15] presented the thermal stress analysis of doubly curved shallow shells using shear flexible finite element method. The basic equations were the extensions of Sanders shell theory to include shear deformation and thermal strains. Obata et al. [16] carried out thermal stresses analysis of a thick hollow cylinder, under two-dimensional temperature distribution. Xing and Liu [17] studied the magneto-thermo-elastic stresses in a conducting rectangular plate subjected to an arbitrary variation of magnetic field using differential quadrature method. Higuchi et al. [18] investigated the magneto-thermo-elastic stress fields induced by a transient magnetic field in an infinite conducting plate and numerically solved the corresponding electromagnetic, thermal and elastic equations. Lee et al. [19] considered three-dimensional axisymmetric coupled magneto-thermo-elasticity problems for laminated circular conical shells subjected to magneto-thermo-elastic loads, using Laplace transform and finite difference methods. Bodaghi and Shakeri [20] carried out an analytical investigation on free vibration and transient response of functionally graded piezoelectric cylindrical panels subjected to impulsive loads. The present work, investigates the three-dimensional problem of an FG truncated conical shell made of non-ferromagnetic metal such as aluminum permeated by a primary uniform magnetic field and subjected to internal pressure and rapid temperature change at the inner surface. The corresponding governing equations in three dimensions are extracted and the differential quadrature approach is applied to discretize the governing equations, boundary conditions and heat conduction equations. Different values of the in-homogeneity constant and inner-wall temperature are used to demonstrate their important roles on the distribution of displacement, stresses, temperature and induced magnetic fields. Results obtained by the present method are validated through comparison with results of the finite element method.

2. GOVERNING EQUATIONS

Consider a three-dimensional conducting truncated conical shell made of FGM, as shown in Figure 1. The

conical shell is referred to the orthogonal coordinate system (s, θ, ζ) with the origin located at the vertex of the complete cone where s is chosen to lay along the generator and on the internal surface, θ is the circumferential coordinate and ζ is taken along the thickness; h_{sh} denotes the thickness of the shell; L and L_1 are the generatrix length and the distance from the vertex to the top surface of the cone, respectively; γ is the semi-vertex angle of the conical shell; R_1 and R_2 represent the inner radii of the cone at its small and large ends, respectively.

The perfectly electro conductive truncated conical shell is assumed to be immersed in a constant magnetic vector field $\vec{H}$ that is uniform along the s and θ directions and acts on the inner surface in ζ direction and subjected to a non-uniform internal pressure $P(\theta)$ that is uniform along generatrix defined by a cosine function. Furthermore, the truncated conical shell is subjected to a rapid temperature change $T(\zeta)$ at the inner surface. The stiffness, magnetic permeability, heat conductivity and thermal expansion coefficients are assumed to vary only through the wall thickness according to the following power law distribution function:

$$Y = Y_0\left(1+\frac{\zeta}{h_{sh}}\right)^n \tag{1}$$

where Y_0 and n represent the material property at the inner surface and the in-homogeneity constant, respectively. Let u, v and w denote corresponding displacement components in s, θ and ζ-directions, respectively. The strain-displacement relations, based on the three-dimensional elasticity formulations and referred to the designated general curvilinear coordinate system are defined as follow [21]:

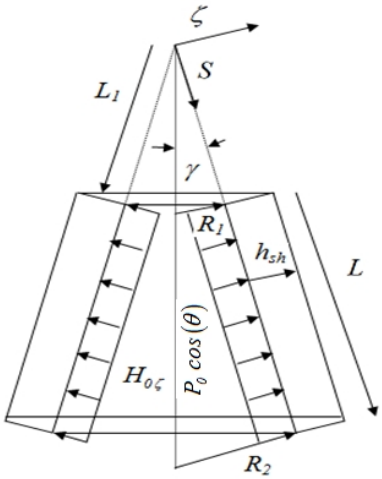

Figure 1. Physical model and system coordinates of the truncated conical shell

$$\begin{aligned}
\varepsilon_{ss} &= \frac{\partial}{\partial s}u+0.5\left(\frac{\partial}{\partial s}w\right)^2\\
\varepsilon_{\theta\theta} &= Z^2\left(\cos(\gamma)\sin(\gamma)uw+0.5\left(\cos(\gamma)^2w^2+\sin(\gamma)^2\right.\right.\\
&\left.u^2+v^2\right)+\sin(\gamma)\left(u\left(\frac{\partial}{\partial\theta}v\right)-v\left(\frac{\partial}{\partial\theta}u\right)\right)+\cos(\gamma)\left(w\left(\right.\right.\\
&\left.\left.\frac{\partial}{\partial\theta}v\right)-v\left(\frac{\partial}{\partial\theta}w\right)\right)\Big)+Z\left(\left(\frac{\partial}{\partial\theta}v\right)+w\cos(\gamma)+u\sin(\gamma)\right)\\
\varepsilon_{\zeta\zeta} &= \frac{\partial}{\partial\zeta}w+0.5\left(\frac{\partial}{\partial\zeta}w\right)^2\\
\varepsilon_{\theta\zeta} &= Z\left(\left(\cos(\gamma)w+\sin(\gamma)u\right)\left(\frac{\partial}{\partial\zeta}v\right)+\left(\left(\frac{\partial}{\partial\theta}w\right)-\cos(\gamma)\right.\right.\\
&\left.v\right)\left(\frac{\partial}{\partial\zeta}w\right)-\cos(\gamma)v-\left(\frac{\partial}{\partial\zeta}u\right)\sin(\gamma)v+\left(\frac{\partial}{\partial\theta}w\right)\Big)+\left(\frac{\partial}{\partial\zeta}v\right)\\
\varepsilon_{s\theta} &= Z\left(\left(\left(\frac{\partial}{\partial\theta}u\right)-\sin(\gamma)v+\left(\frac{\partial}{\partial s}w\right)\left(\frac{\partial}{\partial\theta}w\right)+\left(\frac{\partial}{\partial s}v\right)\left(w\cos(\right.\right.\right.\\
&\left.\left.\gamma)+u\sin(\gamma)\right)-\sin(\gamma)\left(\frac{\partial}{\partial s}u\right)v-\cos(\gamma)\left(\frac{\partial}{\partial s}w\right)v\right)+\left(\frac{\partial}{\partial s}v\right)\\
\varepsilon_{s\zeta} &= \left(\frac{\partial}{\partial\zeta}u\right)+\left(\frac{\partial}{\partial s}w\right)+\left(\frac{\partial}{\partial s}w\right)\left(\frac{\partial}{\partial\zeta}w\right)
\end{aligned} \tag{2}$$

where: $Z = 1/(s\sin(\gamma)+\zeta\cos(\gamma))$

The mechanical constitutive relations which relate components of stress field to components of strain field, ε_{ij} including the thermal effect for an isotropic material in the matrix form are:

$$\begin{bmatrix}\sigma_{ss}\\ \sigma_{\theta\theta}\\ \sigma_{\zeta\zeta}\\ \tau_{\theta\zeta}\\ \tau_{s\zeta}\\ \tau_{s\theta}\end{bmatrix}=\begin{bmatrix}c_{11} & c_{12} & c_{13} & 0 & 0 & 0\\ c_{21} & c_{22} & c_{23} & 0 & 0 & 0\\ c_{31} & c_{32} & c_{33} & 0 & 0 & 0\\ 0 & 0 & 0 & c_{44} & 0 & 0\\ 0 & 0 & 0 & 0 & c_{55} & 0\\ 0 & 0 & 0 & 0 & 0 & c_{66}\end{bmatrix}\begin{bmatrix}\varepsilon_{ss}-\alpha T\\ \varepsilon_{\theta\theta}-\alpha T\\ \varepsilon_{\zeta\zeta}-\alpha T\\ \varepsilon_{\theta\zeta}\\ \varepsilon_{s\zeta}\\ \varepsilon_{s\theta}\end{bmatrix} \tag{3}$$

where σ_{ij} and τ_{ij} represent the Kirchhoff stress components and ε_{ij} represents the strain components, T is the temperature distribution determined from the heat conduction equation and α is the coefficient of thermal expansion.

The material elastic constants of the FG truncated conical shell i.e. $c_{i,j}$, i,j=1, 2, 3, 4, 5, 6 are defined in terms of the elastic module E and the Poisson's ratio υ with the help of two Lame's coefficients λ and G defined as follow:

$$\lambda = \frac{\upsilon E}{(1+\upsilon)(1-2\upsilon)},\quad G = \frac{E}{2(1+\upsilon)} \tag{4}$$

and for the FG truncated conical shell the material elastic constants $c_{i,j}$, i,j=1, 2, 3, 4, 5, 6 which can be obtained from elastic modulus E and Poisson's ratio υ are as follows:

$$c_{11}=\lambda+2G,\ c_{12}=\lambda,\ c_{44}=G,$$
$$c_{12}=c_{21}=c_{13}=c_{31}=c_{32}=c_{23},$$
$$c_{11}=c_{22}=c_{33},\ c_{44}=c_{55}=c_{66} \quad (5)$$

By substituting Equation (2) into Equation (3), components of the stress field are defined in terms of components of the displacement and temperature fields which are given in Appendix A:

The constitutive electromagnetic relations for a perfectly conducting, elastic body neglecting the electric displacement are given in the following form [22]:

$$\vec{J}=\nabla\times\vec{h},\ \nabla\times\vec{e}=-\mu(r)\times\vec{h},\ divh=0,$$
$$\vec{e}=-\mu(r)\times(\vec{U}\times\vec{h}) \quad (6)$$

According to above relations the initial magnetic field vector $\vec{H}$ produces an induced magnetic field $\vec{h}$ and an electric current density vector $\vec{J}$. In order to obtain the induced magnetic field vector $\vec{h}$ from Equation (6), we have to invoke the following relation [23]:

$$curl(\vec{U}\times\vec{H})=\vec{U}\,div(\vec{H})-\vec{H}div(\vec{U})+(\vec{H}.\nabla)\vec{U}-(\vec{U}.\nabla)\vec{H} \quad (7)$$

The terms in Equation (7) can be evaluated using all vector differential operators of gradient, divergence and curl defined in the general conical system (s,θ,ζ). The above mentioned operators for the vector function $X(v_s,v_\theta,v_\zeta)$ are expressed as in Equations (8a) and (8b):

$$div(v)=\frac{\partial v_s}{\partial s}+\frac{\partial v_\zeta}{\partial\zeta}+Z\left(\frac{\partial v_\theta}{\partial\theta}+v_s\sin(\gamma)+v_\zeta\cos(\gamma)\right) \quad (8a)$$

and the Conical-curl-component is:

$$\left(Z\left(\frac{\partial v_\zeta}{\partial\theta}-\frac{\partial}{\partial\zeta}\left(\frac{1}{Z}v_\theta\right)\right),\frac{\partial v_s}{\partial\zeta}-\frac{\partial v_\zeta}{\partial s},Z\left(-\frac{\partial v_s}{\partial\theta}+\frac{\partial}{\partial s}\left(\frac{1}{Z}v_\theta\right)\right)\right) \quad (8b)$$

Applying an initial magnetic field vector $\vec{H}=(0,0,H_{0\zeta})$ that acts in the ζ-direction and the displacement vector $\vec{U}=(u,v,w)$ in conical coordinate system (s,θ,ζ) to Equation (6) and employing Equation (7) results in an approximation of the induced magnetic field and the electric current density vector within the shell:

$$h=(h_s,h_\theta,h_\zeta),h_s=\left(\frac{\partial u}{\partial\zeta}+Z\cos(\gamma)u\right)H_{0\zeta},\quad h_\theta=\left(\frac{\partial v}{\partial\zeta}+Z\cos(\gamma)v(1+Z^2)\right)H_{0\zeta},h_\zeta=-\left(\frac{\partial u}{\partial s}+Z\left(\frac{\partial v}{\partial\theta}+\sin(\gamma)u\right)\right)H_{0\zeta}$$
$$J_s=H_{0\zeta}Z\left(\left(\frac{\partial^2u}{\partial s\partial\theta}+Z\left(\frac{\partial^2v}{\partial\theta^2}+\sin(\gamma)\frac{\partial u}{\partial\theta}\right)\right)-\frac{\partial}{\partial\zeta}\left(Z\left(\frac{\partial v}{\partial\zeta}+A\cos(\gamma)(1+Z^2)\right)v\right)\right)$$
$$J_\theta=H_{0\zeta}\left(\frac{\partial^2u}{\partial s^2}+Z\left(\frac{\partial^2v}{\partial s\partial\theta}+\sin(\gamma)\frac{\partial u}{\partial s}\right)-Z^2(\sin(\gamma)\left(\frac{\partial v}{\partial\theta}+\sin(\gamma)u\right)\right)+\frac{\partial^2u}{\partial\zeta^2}+Z(\cos(\gamma)\frac{\partial u}{\partial\zeta}\Big)-Z^2\left(\cos(\gamma)^2u\right)\Big),$$
$$J_\zeta=H_{0\zeta}Z\left(-\left(\left(\frac{\partial^2u}{\partial\zeta\partial\theta}\right)+Z\left(\cos(\gamma)\frac{\partial u}{\partial\theta}\right)\right)+\frac{\partial}{\partial s}\left(Z\left(\frac{\partial v}{\partial\zeta}+\cos(\gamma)vZ(1+Z^2)\right)H_{0\zeta}\right)\right) \quad (9)$$

The magneto-elastic interactions, subjects the conducting truncated conical shell to the Lorentz's force f_l, which has two components in the s and θ-directions as follows:

$$f_l=\mu\left(\vec{J}\times\vec{H}\right),\ f_l=(f_s,f_\theta,f_\zeta),\ f_s=\mu H_{0\zeta}J_\theta,$$
$$f_\theta=-\mu H_{0\zeta}J_s,\ f_\zeta=0 \quad (10)$$

In the presence of body forces, the stress equilibrium equations in s, θ and ζ -directions are expressed in Equations (11a), (11b) and (11c), respectively as:

$$\frac{\partial}{\partial s}\sigma_{ss}+\frac{\partial}{\partial\zeta}\tau_{s\zeta}+Z\left((\sigma_{ss}-\sigma_{\theta\theta})\sin(\gamma)+\left(\tau_{s\zeta}+\frac{\partial}{\partial\theta}\tau_{s\theta}\right)\cos(\gamma)\right)+f_{s1}=0 \quad (11a)$$

$$\frac{\partial}{\partial s}\tau_{s\theta}+\frac{\partial}{\partial\zeta}\tau_{\zeta\theta}+Z\left(\left(\frac{\partial}{\partial\theta}\sigma_{\theta\theta}\right)+2\tau_{\zeta\theta}\cos(\gamma)+2\tau_{s\theta}\sin(\gamma)\right)+f_\theta=0 \quad (11b)$$

$$\frac{\partial}{\partial s}\tau_{s\zeta}+\frac{\partial}{\partial\zeta}\sigma_{\zeta\zeta}+Z\left(\left(\frac{\partial}{\partial\theta}\tau_{\zeta\theta}\right)+\tau_{s\zeta}\sin(\gamma)+(\sigma_{\zeta\zeta}-\sigma_{\theta\theta})\cos(\gamma)\right)+f_\zeta=0 \quad (11c)$$

Substituting constitutive law as shown in the Appendix and Lorentz's force components of Equation (10) into the equilibrium Equations (11a), (11b) and (11c), a system of equilibrium equations in terms of displacement, thermal and magnetic components in three directions i.e. s, θ and ζ are achieved:

Equilibrium equation in the s-direction can be expressed as:

$$\frac{\partial}{\partial s}\left(\frac{E_0(1+\frac{\zeta}{h_{sh}})^n}{(1+\upsilon)(1-2\upsilon)}\left((1-\upsilon)\left(\frac{\partial}{\partial s}u+0.5\left(\frac{\partial}{\partial s}w\right)^2\right)+\upsilon\right.\right.$$
$$\left(Z^2\left(\cos(\gamma)\sin(\gamma)uw+0.5\left(\cos(\gamma)^2w^2+\sin(\gamma)^2u^2+v^2\right)+\sin(\gamma)\left(\left(\frac{\partial}{\partial\theta}v\right)u-\left(\frac{\partial}{\partial\theta}u\right)v\right)+\cos(\gamma)\left(\left(\frac{\partial}{\partial\theta}v\right)w-\left(\frac{\partial}{\partial\theta}w\right)v\right)\right)+Z\left(\left(\frac{\partial}{\partial\theta}v\right)+w\cos(\gamma)+\sin(\gamma)u\right)\right. \quad (12a)$$

$$+\frac{\partial}{\partial\zeta}w+0.5\left(\frac{\partial}{\partial\zeta}w\right)^2\Big)\Big)\Big)+\frac{\partial}{\partial\zeta}\Bigg(\frac{E_0(1+\frac{\zeta}{h_{sh}})^n}{2(1+\upsilon)}\Big(\Big(\frac{\partial}{\partial\zeta}u\Big)$$

$$+\Big(\frac{\partial}{\partial s}w\Big)+\Big(\frac{\partial}{\partial s}w\Big)\Big(\frac{\partial}{\partial\zeta}w\Big)\Big)\Big)+Z\Bigg(\frac{E_0(1+\frac{\zeta}{h_{sh}})^n(1-2\upsilon)}{(1+\upsilon)(1-2\upsilon)}$$

$$\Big(\frac{\partial}{\partial s}u+0.5\Big(\frac{\partial}{\partial s}w\Big)^2-\Big(Z^2\left(\cos(\gamma)\sin(\gamma)uw+0.5\Big(\cos(\gamma)^2\right.$$

$$w^2+\sin(\gamma)^2u^2+v^2\Big)+\sin(\gamma)\Big(u\Big(\frac{\partial}{\partial\theta}v\Big)-v\Big(\frac{\partial}{\partial\theta}u\Big)\Big)+$$

$$\cos(\gamma)\Big(w\Big(\frac{\partial}{\partial\theta}v\Big)-v\Big(\frac{\partial}{\partial\theta}v\Big)\Big)\Big)+Z\Big(\Big(\frac{\partial}{\partial\theta}v\Big)+w\cos(\gamma)+$$

$$u\sin(\gamma)\Big)\Big)\Big)\sin(\gamma)+\frac{E_0(1+\frac{\zeta}{h_{sh}})^n}{2(1+\upsilon)}\Big(\frac{\partial}{\partial\theta}\Big(Z\Big(\Big(\frac{\partial}{\partial\theta}u\Big)-\sin(\gamma)$$

$$v+\Big(\frac{\partial}{\partial s}w\Big)\Big(\frac{\partial}{\partial\theta}w\Big)+\Big(\frac{\partial}{\partial s}v\Big)\big(\cos(\gamma)w+\sin(\gamma)u\big)-\sin(\gamma)$$

$$\Big(\frac{\partial}{\partial s}u\Big)v-\cos(\gamma)\Big(\frac{\partial}{\partial s}w\Big)v\Big)+\Big(\frac{\partial}{\partial s}v\Big)\Big)+\Big(\frac{\partial}{\partial\zeta}u\Big)+\Big(\frac{\partial}{\partial s}w\Big)$$

$$+\Big(\frac{\partial}{\partial s}w\Big)\Big(\frac{\partial}{\partial\zeta}w\Big)\Big)\cos(\gamma)\Big)=0$$

and the equilibrium equation in the θ- direction can be expressed as:

$$Z\Bigg(\frac{\partial}{\partial\theta}\Bigg(\frac{E_0(1+\frac{\zeta}{h_{sh}})^n}{(1+\upsilon)(1-2\upsilon)}\Big((1-\upsilon)\Big(Z^2\left(\cos(\gamma)\sin(\gamma)uw\right.$$

$$+0.5\Big(\cos(\gamma)^2w^2+\sin(\gamma)^2u^2+v^2\Big)+\sin(\gamma)\Big(\Big(\frac{\partial}{\partial\theta}v\Big)u$$

$$-\Big(\frac{\partial}{\partial\theta}u\Big)v\Big)+\cos(\gamma)\Big(\Big(\frac{\partial}{\partial\theta}v\Big)w-\Big(\frac{\partial}{\partial\theta}w\Big)v\Big)\Big)+Z\Big(\Big(\frac{\partial}{\partial\theta}$$

$$v\Big)+w\cos(\gamma)+u\sin(\gamma)\Big)\Big)+\upsilon\Big(\Big(\frac{\partial}{\partial s}u\Big)+\Big(\frac{\partial}{\partial\zeta}w\Big)+0.5\Big($$

$$\Big(\frac{\partial}{\partial s}w\Big)^2+\Big(\frac{\partial}{\partial\zeta}w\Big)^2\Big)\Big)\Big)\Big)+\frac{E_0(1+\frac{\zeta}{h_{sh}})^n}{(1+\upsilon)}\Big(\Big(Z\Big(\Big(\frac{\partial}{\partial\theta}u\Big)-$$

$$\sin(\gamma)v+\Big(\frac{\partial}{\partial s}w\Big)\Big(\frac{\partial}{\partial\theta}w\Big)+\Big(\frac{\partial}{\partial s}v\Big)\big(\cos(\gamma)w+\sin(\gamma)u\big)$$

$$-\sin(\gamma)\Big(\frac{\partial}{\partial s}u\Big)v-\cos(\gamma)\Big(\frac{\partial}{\partial s}w\Big)v\Big)+\Big(\frac{\partial}{\partial s}v\Big)\Big)\Big)\sin(\gamma)$$

$$+Z\left(\big(\cos(\gamma)w+\sin(\gamma)u\big)\Big(\frac{\partial}{\partial\zeta}v\Big)+\Big(\Big(\frac{\partial}{\partial\theta}w\Big)-\cos(\gamma)v\right)$$

$$\Big(\frac{\partial}{\partial\zeta}w\Big)-\cos(\gamma)v-\sin(\gamma)v\Big(\frac{\partial}{\partial\zeta}u\Big)+\Big(\frac{\partial}{\partial\theta}w\Big)\Big)+\Big(\frac{\partial}{\partial\zeta}v\Big)$$

$$\big)\cos(\gamma)\Big)+\frac{\partial}{\partial\zeta}\Bigg(\frac{E_0(1+\frac{\zeta}{h_{sh}})^n}{2(1+\upsilon)}\Big(Z\Big(\big(\cos(\gamma)w+\sin(\gamma)u\big)\Big($$

$$\Big(\frac{\partial}{\partial\zeta}v\Big)+\Big(\Big(\frac{\partial}{\partial\theta}w\Big)-\cos(\gamma)v\Big)\Big(\frac{\partial}{\partial\zeta}w\Big)-\cos(\gamma)v-\sin(\gamma)v$$

$$\Big(\frac{\partial}{\partial\zeta}u\Big)+\Big(\frac{\partial}{\partial\theta}w\Big)\Big)+\Big(\frac{\partial}{\partial\zeta}v\Big)\Big)\Big)+\frac{\partial}{\partial s}\Bigg(\frac{E_0(1+\frac{\zeta}{h_{sh}})^n}{2(1+\upsilon)}\Big(Z\Big(\Big(\frac{\partial}{\partial\theta}$$

$$u\Big)-\sin(\gamma)v+\Big(\frac{\partial}{\partial s}w\Big)\Big(\frac{\partial}{\partial\theta}w\Big)+\Big(\frac{\partial}{\partial s}v\Big)\big(\cos(\gamma)w+\sin(\gamma)u\big)$$

$$-\sin(\gamma)\Big(\frac{\partial}{\partial s}u\Big)v-\cos(\gamma)\Big(\frac{\partial}{\partial s}w\Big)v\Big)+\Big(\frac{\partial}{\partial s}v\Big)\Big)\Big)=0 \qquad (12b)$$

and finally the equilibrium equation in the ζ- direction is:

$$\frac{E_0(1+\frac{\zeta}{h_{sh}})^n}{2(1+\upsilon)}\frac{\partial}{\partial s}\Big(\Big(\frac{\partial}{\partial\zeta}u\Big)+\Big(\frac{\partial}{\partial s}w\Big)+\Big(\frac{\partial}{\partial s}w\Big)\Big(\frac{\partial}{\partial\zeta}w\Big)\Big)+$$

$$\frac{\partial}{\partial\zeta}\Bigg(\frac{E_0(1+\frac{\zeta}{h})^n}{(1+\upsilon)(1-2\upsilon)}\Big(\upsilon\Big(\frac{\partial}{\partial s}u+0.5\Big(\frac{\partial}{\partial s}w\Big)^2+\Big(Z^2\cos(\gamma)\right.$$

$$\sin(\gamma)uw+0.5\big(\cos(\gamma)^2w^2+\sin(\gamma)^2u^2+v^2\big)+\sin(\gamma)$$

$$\Big(\Big(\frac{\partial}{\partial\theta}v\Big)u-\Big(\frac{\partial}{\partial\theta}u\Big)v\Big)+\cos(\gamma)\Big(\Big(\frac{\partial}{\partial\theta}v\Big)w-\Big(\frac{\partial}{\partial\theta}w\Big)v\Big)\Big)$$

$$+Z\Big(\Big(\frac{\partial}{\partial\theta}v\Big)+\cos(\gamma)w+\sin(\gamma)u\Big)\Big)+(1-\upsilon)\Big(\frac{\partial}{\partial\zeta}w+0.5$$

$$\Big(\frac{\partial}{\partial\zeta}w\Big)^2\Big)\Big)\Big)+Z\Bigg(\frac{\partial}{\partial\theta}\Bigg(\frac{E_0(1+\frac{\zeta}{h_{sh}})^n}{2(1+\upsilon)}\Big(Z\Big(\big(\cos(\gamma)w+\sin(\gamma)\right.$$

$$u\Big)\Big(\frac{\partial}{\partial\zeta}v\Big)+\Big(\Big(\frac{\partial}{\partial\theta}w\Big)-\cos(\gamma)v\Big)\Big(\frac{\partial}{\partial\zeta}w\Big)-\cos(\gamma)v-\sin(\gamma)$$

$$v\Big(\frac{\partial}{\partial\zeta}u\Big)+\Big(\frac{\partial}{\partial\theta}w\Big)\Big)+\Big(\frac{\partial}{\partial\zeta}v\Big)\Big)\Big)+\sin(\gamma)\frac{E_0(1+\frac{\zeta}{h_{sh}})^n}{2(1+\upsilon)}\Big(\Big(\frac{\partial}{\partial\zeta}$$

$$u\Big)+\Big(\frac{\partial}{\partial s}w\Big)+\Big(\frac{\partial}{\partial s}w\Big)\Big(\frac{\partial}{\partial\zeta}w\Big)\Big)+\cos(\gamma)\frac{E_0(1+\frac{\zeta}{h_{sh}})^n(2\upsilon-1)}{(1+\upsilon)(1-2\upsilon)}$$

$$\Big(Z^2\left(\cos(\gamma)\sin(\gamma)uw+0.5\big(\cos(\gamma)^2w^2+\sin(\gamma)^2u^2+v^2\big)+\right. \qquad (12c)$$

$$\sin(\gamma)\Big(\Big(\frac{\partial}{\partial\theta}v\Big)u-\Big(\frac{\partial}{\partial\theta}u\Big)v\Big)+\cos(\gamma)\Big)\Big(\Big(\frac{\partial}{\partial\theta}v\Big)w-\Big(\frac{\partial}{\partial\theta}w\Big)$$

$$v\Big)\Big)+Z\Big(\Big(\frac{\partial}{\partial\theta}v\Big)+\cos(\gamma)w+\sin(\gamma)u\Big)-\Big(\frac{\partial}{\partial\zeta}w+0.5\Big(\frac{\partial}{\partial\zeta}w\Big)^2$$

$$\left.\left.\left.\Big)\Big)\Big)=0\right.\right.$$

The FG truncated conical shell is assumed to be subjected to a non-uniform pressure $P(\theta)$, at the inner surface, the boundary temperature (T_i) and permeated by the initial condition of magnetic field, $H_{0\zeta}$. It is also supposed that the outer surface of the shell is traction free with its temperature (T_o) being kept at 0^o. For the

sake of simplicity, the initial conditions are expressed as:

$$\begin{aligned}&\zeta=0,\ \sigma_{rr}=P_0\cos(\theta),\ \tau_{s\zeta}=0,\ \tau_{\theta\zeta}=0,\ T_i=T,\ H=H_{O\zeta}\\&\zeta=h_{sh},\ \sigma_{rr}=0,\ \tau_{s\zeta}=0,\ \tau_{\theta\zeta}=0,\ T_O=0,\ H=0\end{aligned}\tag{13}$$

Moreover, top and bottom surfaces are assumed to be clamped, hence boundary conditions at these surfaces are expressed as:

$$\begin{aligned}&s=\frac{R_1}{\sin(\gamma)},\ u=0,\ w=0,\ v=0,\ T_t=0\\&s=\frac{R_1}{\sin(\gamma)}+L,\ u=0,\ w=0,\ v=0,\ T_b=0\end{aligned}\tag{14}$$

The temperature distribution can be determined by solving the steady-state heat conduction equation for the FGM truncated conical shell through the thickness that is given by:

$$\begin{aligned}&\left(\frac{K\cos(\gamma)}{R_1+s\sin(\gamma)+\zeta\cos(\gamma)}\right)\frac{\partial}{\partial\zeta}T+K\frac{\partial^2T}{\partial\zeta^2}+\frac{\partial}{\partial\zeta}K\\&\frac{\partial}{\partial\zeta}T=0\end{aligned}\tag{15}$$

where K is the coefficient of heat conductivity.

3. THE METHOD OF SOLUTION

The differential quadrature method as a powerful semi-analytical tool is employed to obtain the discretized forms governing and boundary equations of the conical shell. The general rule of DQM postulates that derivatives of any smooth function at a discrete point in the domain can be expressed as a weighted linear summation of all the functional values at all discrete sampling points. The key to DQM is to determine the weighting coefficients for discretization of a derivative of any order.

The n^{th} order derivative of a function $F(x)$ at any discrete point of a domain with respect to s, θ and ζ at any sampling point i.e. s_i, θ_i and ζ_i are explicitly expressed as [24]:

$$\begin{aligned}&\frac{\partial}{\partial\zeta}f=\sum_{n=1}^{N}A^{(1)}_{k,n}f_{i,j,n},\ \frac{\partial^2f}{\partial\zeta^2}=\sum_{n=1}^{N}A^{(2)}_{k,n}f_{i,j,n}\\&\frac{\partial}{\partial s}f=\sum_{l=1}^{P}B^{(1)}{}_{i,l}f_{l,j,k},\ \frac{\partial^2f}{\partial s^2}=\sum_{l=1}^{P}B^{(2)}{}_{i,l}f_{l,j,k}\\&\frac{\partial}{\partial\theta}f=\sum_{m=1}^{M}C^{(1)}{}_{j,m}f_{j,m,k},\ \frac{\partial^2f}{\partial\theta^2}=\sum_{m=1}^{M}C^{(2)}{}_{j,m}f_{i,m,k}\\&\frac{\partial^2f}{\partial s\partial\theta}=\sum_{m=1}^{M}\sum_{l=1}^{P}C_{j,m}B_{i,l}f_{l,m,k},\ \frac{\partial^2f}{\partial s\partial\zeta}=\sum_{n=1}^{N}\sum_{l=1}^{P}A_{k,n}C_{i,l}f_{l,j,n},\\&\frac{\partial^2f}{\partial\theta\partial\zeta}=\sum_{n=1}^{N}\sum_{m=1}^{M}A_{k,n}B_{j,m}f_{i,m,n}\end{aligned}\tag{16}$$

where $A^{(n)}$ are weighting coefficients for the n^{th}-order derivative at point ζ_i along the thickness direction; $B^{(n)}$ are weighting coefficients for the n^{th}-order derivative at point s_i along the generator and $C^{(n)}$ are weighting coefficients for the n^{th}-order derivative at point θ_i in the circumferential direction; P, M and N are numbers of sampling points along the s, θ and ζ, respectively .The computation of weighting coefficients in s and ζ-directions have been made on the basis of polynomial differential qaudrature (PDQ) and in circumferential direction using the Fourier Expansion-based differential quadrature (FDQ) which are defined in Equations (17a) and (17b), respectively:

$$\begin{aligned}&A^{(1)}_{i,j}=\frac{1}{x_j-x_i}\prod_{\substack{k=1\\k\neq i,j}}^{N}\frac{x_i-x_k}{x_j-x_k},\ i\neq j,\ A^{(1)}_{i,i}=\sum_{\substack{k=1\\k\neq i}}^{N}\frac{1}{x_i-x_k},\\&A^{(2)}_{i,j}=\sum_{k=1}^{N}A^{(1)}_{i,k}A^{(1)}_{k,j}\end{aligned}\tag{17a}$$

$$\begin{aligned}&C_{ij}=\frac{q(x_i)}{2\sin(\frac{x_i-x_j}{2})q(x_j)},\ i\neq j,\ q(x_i)=\prod_{k=0}^{M}\sin(\frac{x_i-x_k}{2}),\\&C_{ii}=-\sum_{\substack{j=0\\i\neq j}}^{M}C_{ij},\ C^{(1)}{}_{ij}=C_{ij}(2C_{ii}-\cot(\frac{x_i-x_j}{2})),\ i\neq j\\&,\ C^{(1)}{}_{ii}=-\sum_{\substack{j=0\\i\neq j}}^{M}C^{(1)}{}_{ij},\ C^{(2)}_{i,j}=\sum_{j=0}^{M}C^{(1)}_{j,m}C^{(1)}_{m,j}\end{aligned}\tag{17b}$$

By substituting the relations in Equation (16) into resulting equations, the following discretized governing, heat conduction and related boundary equations are transformed into a set of algebraic equations. The detailed discretized forms of governing, mechanical boundary and heat transfer equations are given in Appendix A.

4. NUMERICAL RESULTS AND DISCUSSION

Based on the Chebyshev-Gauss-Lobatto formula, sampling points are obtained as follows:
in s- direction:

$$s_i=L_1+\frac{L}{2}(1-\cos(\frac{i-1}{P-1}\pi)),\ i=1,..,P\tag{18}$$

in θ-direction:

$$\theta_j=\frac{j-1}{M}2\pi,\ \ j=1,..,M\tag{19}$$

in ζ-direction:

$$\zeta_i=\frac{h_{sh}}{2}(1-\cos(\frac{i-1}{N-1}\pi)),\ i=1,..,N\tag{20}$$

Geometrical parameters of the shell are considered to be $L=1,\ \gamma=15^0,\ h_{sh}=0.2,\ R_2=0.5$ for the truncated

conical shell. The shell is made of Aluminum with material properties as shown in Equation (21) [25]:

$$E = 70Gpa, \nu = 0.33,\ \alpha_0 = 24\times10^{-6}1/{}^0C,$$
$$\mu_0 = 4\pi\times10^{-7}\ H/m,\ K_0 = 92.6\times10^{-6}\ W/m^0C \quad (21)$$

The shell is assumed to be under the action of the internal pressure $P_0 = 150\cos(\theta)$ MPa and the initiail magnetic field $H_0 = 5\times10^8$ A/m.

The following non-dimensional values are employed to simplify calculations and present the results in a more appropriate form:

$$\bar{\zeta} = \frac{\zeta}{h_{sh}},\ \bar{w} = \frac{w}{h_{sh}},\ \bar{T} = \frac{T}{T_i},\ \bar{\sigma}_{\zeta\zeta} = \frac{\sigma_{\zeta\zeta}}{P_0},\ \bar{\sigma}_{\theta\theta} = \frac{\sigma_{\theta\theta}}{P_0},$$
$$\bar{h} = \frac{h}{H_{0\zeta}},\ \bar{\tau}_{\zeta\theta} = \frac{\tau_{\zeta\theta}}{P_0} \quad (22)$$

The effect of variation of the in-homogeneity constant, *n,* on the material properties of the cone i.e. Y_{out}/Y_0 is shown in Figure 2., where Y_{out} and Y_0 are the material properties of the shell at the outer and the inner boundaries of the shell, respectively.

The convergence and accuracy of the present approach is investigated in Figure 3. Numerical results for the distribution of non-dimensional displacement component, $\bar{W}$ through the shell thickness in case of axisymmetric loading condition for various number of grid points along the thickness and the generator are demonstrated. According to the presented results, converged results are achieved using total number of $N\times P = 12$ discrete points. As it can be seen, this method converges quite fast with considerably lower number of grid points. On the other hand, results obtained by the present method are verified with results obtained using the finite element software ANSYS, as illustrated in Figure 3. In the axisymmetric case, the truncated conical shell is modeled and meshed with Solid5 element that has eight nodes with up to six degrees of freedom per node and has 3-D magnetic, thermal and structural field capabilities with limited coupling between them. As it is observed, an excellent agreement exists between the results of the proposed method and the finite element method.

Results obtained for the circumferential distribution of the non-dimensional through thickness components of displacement, $\bar{W}$ and the stress, $\bar{\sigma}_{\zeta\zeta}$ for *n*=0 using the DQ and FE methods are shown and compared in Figures 4 and 5, respectively. It can be concluded from theses figures that these results are in very good agreement. Effects of in-homogeneity constant, *n,* on the dimensionless component of displacement field $\bar{W}$, stress components, the induced magnetic field vector and temperature distributions along the circumferential direction are demonstrated in Figures 6 to 11. In these calculations *n,* varies from -2 to 2. Figure 6 presents the distribution of non-dimensional displacement component, $\bar{W}$ with various values of in-homogeneity constant along the circumferential direction. Results revealed that by changing *n,* from positive to negative the absolute value of $\bar{W}$, increases. The highest amplitude level belongs to $n = -2$ and the lowest one belongs to $n = 2$. It can further be observed from Figure 6 that all curves intersect at some specific positions i.e. $\theta\ \ \pi/2$ and $3\pi/2$ .In Figure 7 variations of $\bar{\sigma}_{\zeta\zeta}$ in the circumferential direction with different values of in-homogeneity constant for an FG truncated conical shell is depicted. It can be seen that by changing the value of *n,* from positive to negative, the value of stress through the thickness $\bar{\sigma}_{\zeta\zeta}$, decreases. A careful study of results shown in Figure 7 will assist designers to strengthen a shell made of non-homogeneous material against the internal pressure and magnetic field by selecting an appropriate inhomogeneous constant.

Variations of the circumferential stress along the circumference with variation of *n* from -2 to 2 are shown in Figure 8. It can be readily seen that as *n* changes from positive to negative, the value of stress reduces and the distribution tends to be more uniform along the circumferential direction. It appears that the in-homogeneity constant has significant effects on the circumferential stress. The behavior of shear stress $\bar{\tau}_{\zeta\theta}$ distribution of an FG truncated conical shell along θ, with different values of in-homogeneity constant *n,* is depicted in Figure 9. It is observed that the absolute value of shear stress $\bar{\tau}_{\zeta\theta}$ gently increases as *n,* changes from positive to negative which implies that it is much less dependent to the value of *n.* It can also be noted that the maximum shear stress $\bar{\tau}_{\zeta\theta}$ occurs at $\theta\ \ \pi/2$ and $3\pi/2$. Figure 10 illustrates the influence of *n,* on the distribution of the induced magnetic field along circumferential direction. As it is shown from the figure, as *n* changes from negative to positive, the absolute value of amplitude of the magnetic induction decreases and produce more uniform curve. It can be concluded that there is substantial influence of the in-homogeneity constant on the induced magnetic field. Figure 11 is plotted to show the variation of temperature along the thickness of the shell for different values of *n.* It is shown in the figure that as *n,* changes from -2 to 2, the temperature amplitude decreases. It is also found that for *n*=0, the temperature distribution is in linear form and for other values of *n* it has a parabolic shape. Stress components resulted from thermal fields play a great role in the fatigue crack initiation, rapid fracture of components causing failure of components at stress levels much below the nominal strength of the material.

Thermal load effects on various parameters of the shell are performed and results are shown in Figures 12 to 16. It is assumed that the in-homogeneity constant is equal to 1, i.e. n=1 and the outer surface temperature is kept at zero with T_i=10 ^{0}C, 170 ^{0}C and 350 ^{0}C. Figure 12 shows the distribution of non-dimensional displacement component, $\overline{W}$ at the middle section of generator of the cone ($s = L_1 + L/2$) in the circumferential direction with different values of the inner-wall temperature. It is observed that as the temperature difference between two surfaces increases, the dimensionless displacement component, $\overline{W}$ increases. Figure 13 shows the effect of uniform temperature rise of the inner surface of an FG truncated conical shell on the distribution of stress component, $\overline{\sigma}_{\zeta\zeta}$ by keeping the outer surface temperature at zero. As it is expected, increasing the temperature difference increases the magnitude of stress $\overline{\sigma}_{\zeta\zeta}$. Distribution of the circumferential stress with different values of the inner-wall temperature along the circumference is shown in Figure 14. It is observed form the figure that as the temperature of the inner surface increases the circumferential stress increases. Since, the thermal effect strongly dominates the values of circumferential stress, usage of FGMs to increase impact resistance and resistance to thermal stress fractures is necessary and vital in appropriate designing of structural components. Figure 15 depicts the effect of the thermal field on the shear stress $\overline{\tau}_{\zeta\theta}$ for the FG truncated conical shell. It can be inferred from the figure that the corresponding response curves are overlapping. This low degree of dependency of the shear stress component $\overline{\tau}_{\zeta\theta}$, to the thermal field are observed in the corresponding thermo-elastic formula which are given in Appendix A. The influence of the thermal field on the variation of the induced magnetic field is shown in Figure 16. The trend is observed to be similar to that of Figures 13 and 15 which means that the influence of temperature difference is noticeable in the induction of magnetic field within the shell. As the value of temperature of the inner-wall increases, the value induced magnetic field significantly increases.

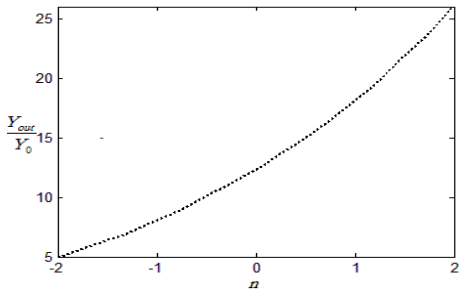

Figure 2. Variation of Y_{out} / Y_O versus n

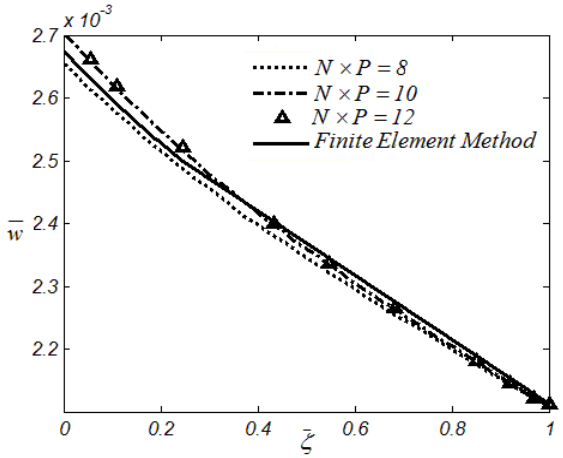

Figure 3. Convergence study of DQ method , variation of $\overline{W}$ with number of grid points; FEM and DQM

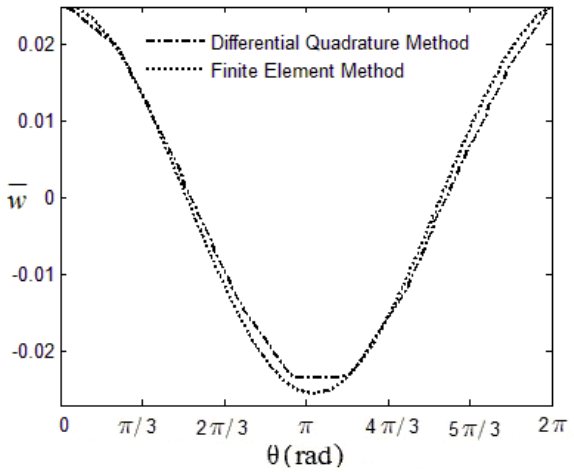

Figure 4. Circumferential distribution of $\overline{W}$, FEM versus DQM

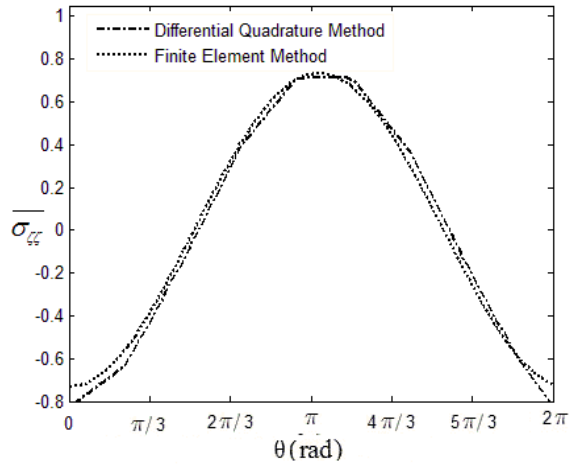

Figure 5. Circumferential distribution of $\overline{\sigma}_{\zeta\zeta}$, FEM versus DQM

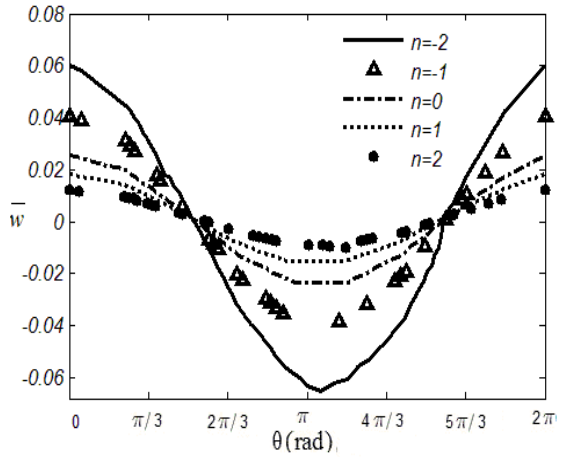

Figure 6. Variation of $\overline{w}$ with *n*, in the circumferential direction

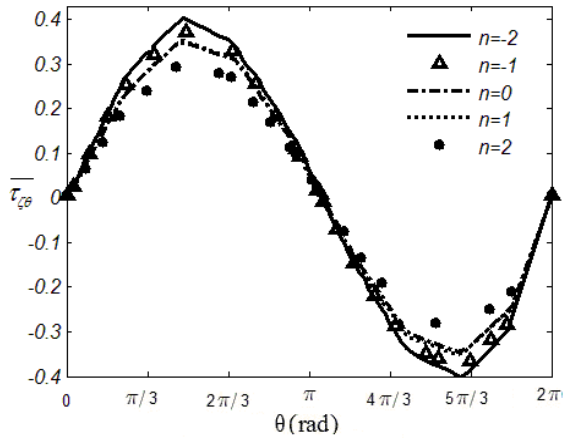

Figure 9. Variation of $\overline{\tau}_{\zeta\theta}$ with *n*, in the circumferential direction

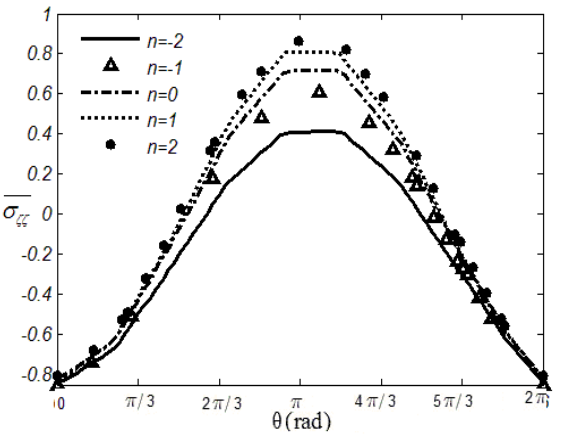

Figure 7. Variation of $\overline{\sigma}_{\zeta\zeta}$ with *n*, in the circumferential direction

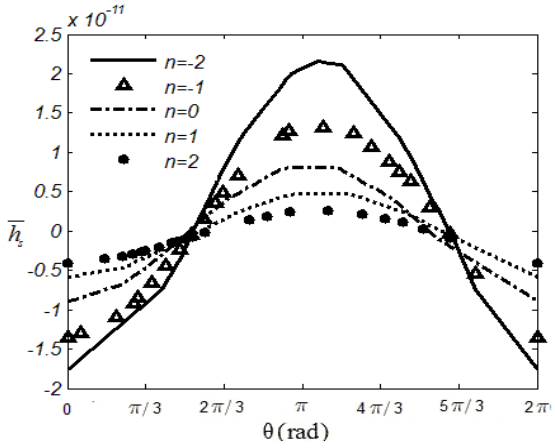

Figure 10. Variation of $\overline{h}$ with *n*, in the circumferential direction

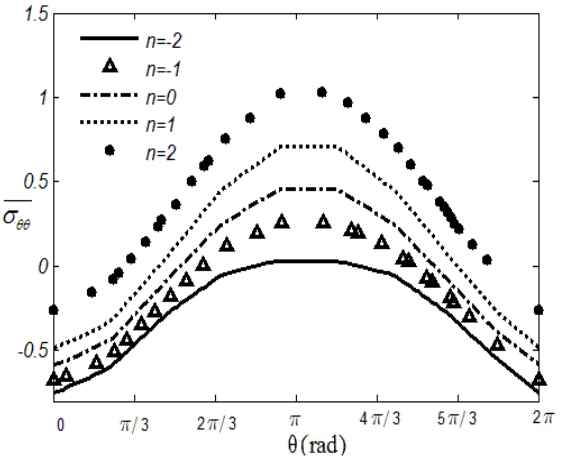

Figure 8. Variation of $\overline{\sigma}_{\theta\theta}$ with *n*, in the circumferential direction

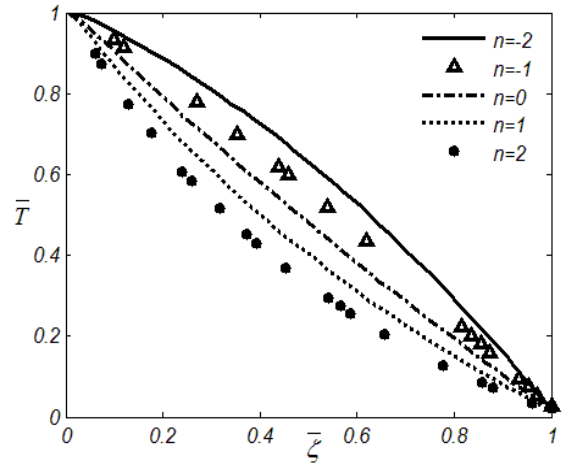

Figure 11. Variation of $\overline{T}$ with *n*, in the circumferential direction

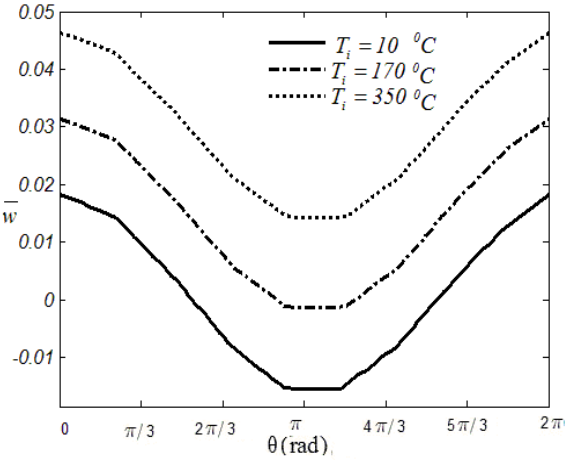

Figure 12. Thermal load effect on variation of $\overline{w}$ in the circumferential direction

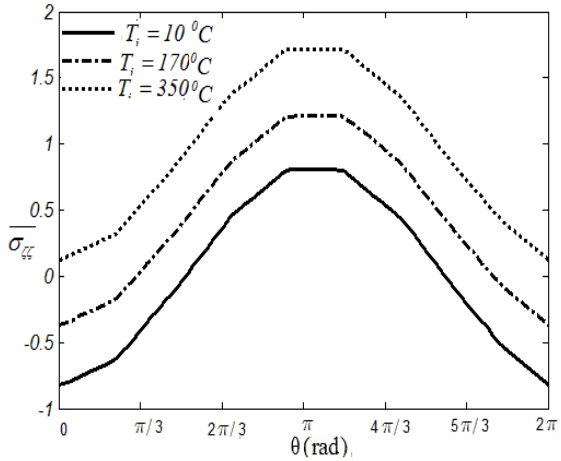

Figure 13 .Thermal load effect on variation of $\overline{\sigma}_{\zeta\zeta}$ in the circumferential direction

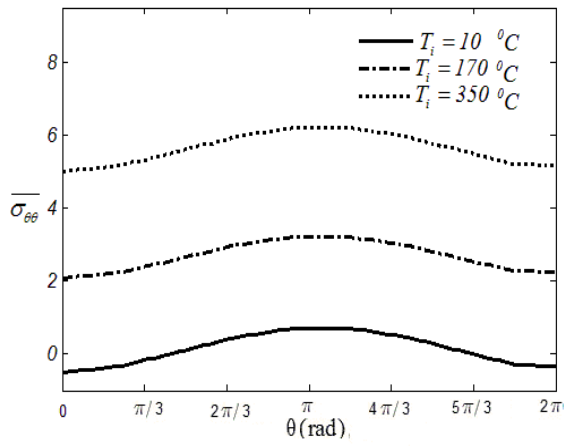

Figure 14. Thermal load effect on variation of $\overline{\sigma}_{\theta\theta}$ in circumferential direction

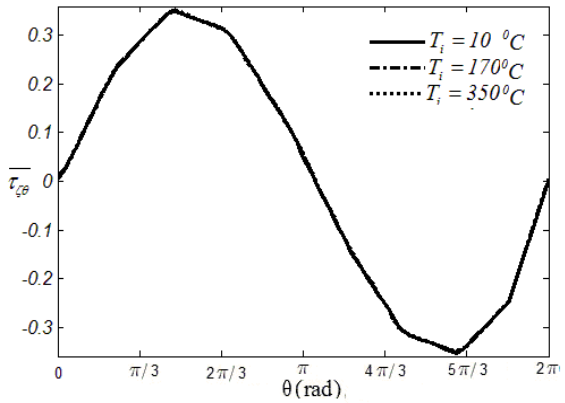

Figure 15. Thermal load effect on variation of $\overline{\tau}_{\zeta\theta}$ in the circumferential direction

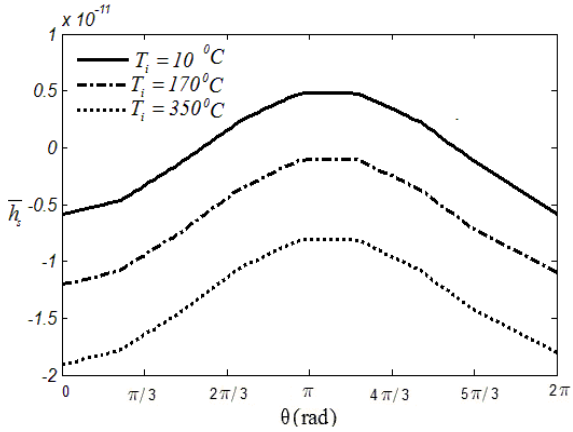

Figure 16. Thermal load effect on variation of $\overline{h}$ in the circumferential direction

5. CONCLUSION

The three-dimensional magneto-thermo-elastic problem of an FG truncated conical shell made of perfect conducting material in the presence of a constant initial magnetic field and subjected to thermal and mechanical loads is investigated in details. Characteristic parameters including the mechanical, magnetic and thermal properties are assumed to vary as function of the thickness and according to a power law formulation. The governing equations of the conical shell are derived and discretized with the help of the semi-analytical differential quadrature method. It is observed that results obtained by DQ method converge to very accurate numerical results using considerably small number of grid points and hence requiring relatively little computational effort. Numerical results were also obtained for different values of the non-homogeneity property of the material and the inner-wall temperature to demonstrate their high effects on the behavior of the

normalized displacement, stress, thermal and induced magnetic fields. By observing the numerical results, it appears that optimum way of designing can be performed by selecting an appropriate non-homogeneity constant, *n*. For instance, changing the non-homogeneity constant from negative to positive, causes the stress components along the circumference and the thickness of the shell to have smaller amplitudes.

6. REFERENCES

1. Higuchi, M., Kawamura, R. and Tanigawa, Y., "Dynamic and quasi-static behaviors of magneto-thermo-elastic stresses in a conducting hollow circular cylinder subjected to an arbitrary variation of magnetic field", ***International Journal of Mechanical Sciences***, Vol. 50, No. 3, (2008), 365-379.
2. Farid, M., Zahedinejad, P. and Malekzadeh, P., "Three-dimensional temperature dependent free vibration analysis of functionally graded material curved panels resting on two-parameter elastic foundation using a hybrid semi-analytic, differential quadrature method", ***Materials & Design***, Vol. 31, No. 1, (2010), 2-13.
3. Shadmehri, F., Hoa, S. and Hojjati, M., "Buckling of conical composite shells", ***Composite Structures***, Vol. 94, No. 2, (2012), 787-792.
4. Sofiyev, A., Zerin, Z. and Korkmaz, A., "The stability of a thin three-layered composite truncated conical shell containing an fgm layer subjected to non-uniform lateral pressure", ***Composite Structures***, Vol. 85, No. 2, (2008), 105-115.
5. Xu, C., Xia, Z. and Chia, C., "Non-linear theory and vibration analysis of laminated truncated, thick, conical shells", ***International Journal of Non-Linear Mechanics***, Vol. 31, No. 2, (1996), 139-154.
6. Patel, B., Shukla, K. and Nath, Y., "Nonlinear thermoelastic stability characteristics of cross-ply laminated oval cylindrical/conical shells", ***Finite Elements in Analysis and Design***, Vol. 42, No. 12, (2006), 1061-1070.
7. Zhang, J. and Li, S., "Dynamic buckling of fgm truncated conical shells subjected to non-uniform normal impact load", ***Composite Structures***, Vol. 92, No. 12, (2010), 2979-2983.
8. Aghdam, M., Shahmansouri, N. and Bigdeli, K., "Bending analysis of moderately thick functionally graded conical panels", ***Composite Structures***, Vol. 93, No. 5, (2011), 1376-1384.
9. Wu, C.-P., Pu, Y.-F. and Tsai, Y.-H., "Asymptotic solutions of axisymmetric laminated conical shells", ***Thin-Walled Structures***, Vol. 43, No. 10, (2005), 1589-1614.
10. Petrovic, A., "Stress analysis in cylindrical pressure vessels with loads applied to the free end of a nozzle", ***International Journal of Pressure Vessels and Piping***, Vol. 78, No. 7, (2001), 485-493.
11. Jabbari, M., Sohrabpour, S. and Eslami, M., "Mechanical and thermal stresses in a functionally graded hollow cylinder due to radially symmetric loads", ***International Journal of Pressure Vessels and Piping***, Vol. 79, No. 7, (2002), 493-497.
12. Eslami, M., Babaei, M. and Poultangari, R., "Thermal and mechanical stresses in a functionally graded thick sphere", ***International Journal of Pressure Vessels and Piping***, Vol. 82, No. 7, (2005), 522-527.
13. Paliwal, D. and Sinha, S., "Static and dynamic behaviour of shallow spherical shells on winkler foundation", ***Thin-Walled Structures***, Vol. 4, No. 6, (1986), 411-422.
14. Jane, K. and Wu, Y., "A generalized thermoelasticity problem of multilayered conical shells", ***International Journal of Solids and Structures***, Vol. 41, No. 9, (2004), 2205-2233.
15. Chandrashekhara, K. and Bhimaraddi, A., "Thermal stress analysis of laminated doubly curved shells using a shear flexible finite element", ***Computers & Structures***, Vol. 52, No. 5, (1994), 1023-1030.
16. Obata, Y., Kanayama, K., Ohji, T. and Noda, N., "Two-dimensional unsteady thermal stresses in a partially heated circular cylinder made of functionally graded material", ***Proc Therm Stress***, Vol. 99, (1999), 13-17.
17. Xing, Y. and Liu, B., "A differential quadrature analysis of dynamic and quasi-static magneto-thermo-elastic stresses in a conducting rectangular plate subjected to an arbitrary variation of magnetic field", ***International Journal of Engineering Science***, Vol. 48, No. 12, (2010), 1944-1960.
18. Higuchi, M., Kawamura, R., Tanigawa, Y. and Fujieda, H., "Magnetothermoelastic stresses induced by a transient magnetic field in an infinite conducting plate", ***Journal of Mechanics of Materials and Structures,*** Vol. 2, (2007), 113-130.
19. Lee, Z.-Y., Wu, Y.-H., Sung, H.-M. and Wang, C.-C., "Magnetothermoelastic transient response of multilayered conical shells", ***International Communications in Heat and Mass Transfer***, Vol. 35, No. 9, (2008), 1113-1124.
20. Bodaghi, M. and Shakeri, M., "An analytical approach for free vibration and transient response of functionally graded piezoelectric cylindrical panels subjected to impulsive loads", ***Composite Structures***, Vol. 94, No. 5, (2012), 1721-1735.
21. Chung, T., "General continuum mechanics", Cambridge University Press Cambridge, (2007).
22. Kraus, J. D. and Fleisch, D. A., "Electromagnetics", McGraw-Hill New York, (1984).
23. Strang, G. and Aarikka, K., "Introduction to applied mathematics", Wellesley-Cambridge Press Wellesley, MA, Vol. 16, (1986).
24. Shu, C., "Differential quadrature: And its application in engineering", Springer, (2000).
25. Higuchi, M., Kawamura, R. and Tanigawa, Y., "Magneto-thermo-elastic stresses induced by a transient magnetic field in a conducting solid circular cylinder", ***International Journal of Solids and Structures***, Vol. 44, No. 16, (2007), 5316-5335.

APPENDIX A

The stress field in terms of components of the displacement and temperature fields:

$$\sigma_{ss}=c_{11}\left(\frac{\partial}{\partial s}u+0.5\left(\frac{\partial}{\partial s}w\right)^2-\alpha T\right)+c_{12}\left(Z^2\ (\cos(\gamma)\ \sin(\gamma)uw\right.$$
$$+0.5\left(\cos(\gamma)^2w^2+\sin(\gamma)^2u^2+v^2\right)+\sin(\gamma)\left(u\left(\frac{\partial}{\partial\theta}v\right)-v\left(\frac{\partial}{\partial\theta}u\right)\right)$$
$$+\cos(\gamma)\left(w\left(\frac{\partial}{\partial\theta}v\right)-v\left(\frac{\partial}{\partial\theta}w\right)\right)+Z\left(\left(\frac{\partial}{\partial\theta}v\right)+w\cos(\gamma)\right.$$
$$\left.\left.+u\sin(\gamma)\right)\right)+c_{13}\left(\frac{\partial}{\partial\zeta}w+0.5\left(\frac{\partial}{\partial\zeta}w\right)^2-\alpha T\right)$$
$$\sigma_{\theta\theta}=c_{21}\left(\frac{\partial}{\partial s}u+0.5\left(\frac{\partial}{\partial s}w\right)^2-\alpha T\right)+c_{22}\left(Z^2\ (\cos(\gamma)\right.$$
$$\sin(\gamma)uw+0.5\left(\cos(\gamma)^2w^2+\sin(\gamma)^2u^2+v^2\right)+\sin(\gamma)$$
$$\left(u\left(\frac{\partial}{\partial\theta}v\right)-v\left(\frac{\partial}{\partial\theta}u\right)\right)+\cos(\gamma)\left(w\left(\frac{\partial}{\partial\theta}v\right)-v\left(\frac{\partial}{\partial\theta}w\right)\right)$$
$$+Z\left(\left(\frac{\partial}{\partial\theta}v\right)+w\cos(\gamma)+u\sin(\gamma)\right)\right)+c_{23}\left(\frac{\partial}{\partial\zeta}w\right.$$
$$\left.+0.5\left(\frac{\partial}{\partial\zeta}w\right)^2-\alpha T\right)$$
$$\sigma_{\zeta\zeta}=c_{31}\left(\frac{\partial}{\partial s}u+0.5\left(\frac{\partial}{\partial s}w\right)^2-\alpha T\right)+c_{32}\left(Z^2\ (\cos(\gamma)\right.$$
$$\sin(\gamma)uw+0.5\left(\cos(\gamma)^2w^2+\sin(\gamma)^2u^2+v^2\right)+\sin(\gamma)$$
$$\left(u\left(\frac{\partial}{\partial\theta}v\right)-v\left(\frac{\partial}{\partial\theta}u\right)\right)+\cos(\gamma)\left(w\left(\frac{\partial}{\partial\theta}v\right)-v\left(\frac{\partial}{\partial\theta}w\right)\right)$$
$$+Z\left(\left(\frac{\partial}{\partial\theta}v\right)+w\cos(\gamma)+u\sin(\gamma)\right)\right)+c_{33}\left(\frac{\partial}{\partial\zeta}w\right.$$
$$\left.+0.5\left(\frac{\partial}{\partial\zeta}w\right)^2-\alpha T\right)$$
$$\tau_{\zeta\theta}=c_{44}\left(Z\left(\left(\cos(\gamma)w+\sin(\gamma)u\right)\left(\frac{\partial}{\partial\zeta}v\right)+\left(\left(\frac{\partial}{\partial\theta}w\right)-\cos(\gamma)v\right)\right.\right.$$
$$\left.\left.\left(\frac{\partial}{\partial\zeta}w\right)-\cos(\gamma)v-\left(\frac{\partial}{\partial\zeta}u\right)\sin(\gamma)v+\left(\frac{\partial}{\partial\theta}w\right)\right)+\left(\frac{\partial}{\partial\zeta}v\right)\right)$$
$$\tau_{s\zeta}=c_{55}\left(\left(\frac{\partial}{\partial\zeta}u\right)+\left(\frac{\partial}{\partial s}w\right)+\left(\frac{\partial}{\partial s}w\right)\left(\frac{\partial}{\partial\zeta}w\right)\right)$$
$$\tau_{s\theta}=c_{66}\left(Z\left(\left(\frac{\partial}{\partial\theta}u\right)-\sin(\gamma)v+\left(\frac{\partial}{\partial s}w\right)\left(\frac{\partial}{\partial\theta}w\right)+\right.\right.$$
$$\left.\left.\left(\frac{\partial}{\partial s}v\right)\left(\cos(\gamma)w+\sin(\gamma)u\right)-\sin(\gamma)\left(\frac{\partial}{\partial s}u\right)v-\cos\right.\right.$$
$$\left.\left.(\gamma)\left(\frac{\partial}{\partial s}w\right)v\right)+\left(\frac{\partial}{\partial s}v\right)\right)\qquad A_1$$

The DQ form of the equilibrium equation in *s*- direction is presented as follow:

$$\frac{E_9(1+\frac{\zeta_i}{h_{sh}})^n}{(1+\upsilon)(1-2\upsilon)}\left((1-\upsilon)\left(\sum_{l=1}^{P}B^{(2)}{}_{i,l}u_{l,j,k}+\left(\sum_{l=1}^{P}B^{(1)}{}_{i,l}w_{l,j,k}\right)\right.\right.$$
$$\left.\left(\sum_{l=1}^{P}B^{(2)}{}_{i,l}w_{l,j,k}\right)\right)+\upsilon\left(-2\sin(\gamma)Z^3\left(\cos(\gamma)\sin(\gamma)u_{i,j,k}w_{i,j,k}\right.\right.$$
$$+0.5\left(\cos(\gamma)^2w_{i,j,k}{}^2+\sin(\gamma)^2u_{i,j,k}{}^2+v_{i,j,k}{}^2\right)+\sin(\gamma)\left(u_{i,j,k}\right.$$
$$\left.\left(\sum_{m=1}^{M}C^{(1)}{}_{j,m}v_{j,m,k}\right)-v_{i,j,k}\left(\sum_{m=1}^{M}C^{(1)}{}_{j,m}u_{j,m,k}\right)\right)+\cos(\gamma)\left(w_{i,j,k}\right.($$
$$\left.\left.\left.\sum_{m=1}^{M}C^{(1)}{}_{j,m}v_{j,m,k}\right)-v_{i,j,k}\left(\sum_{m=1}^{M}C^{(1)}{}_{j,m}w_{j,m,k}\right)\right)\right)+Z^2\left(\cos(\gamma)\sin(\gamma)\right.$$
$$\left(\left(\sum_{l=1}^{P}B^{(1)}{}_{i,l}u_{l,j,k}\right)w_{i,j,k}+\left(\sum_{l=1}^{P}B^{(1)}{}_{i,l}w_{l,j,k}\right)u_{i,j,k}\right)+\cos(\gamma)^2\left(\sum_{l=1}^{P}\right.$$
$$\left.B^{(1)}{}_{i,l}w_{l,j,k}\right)w_{i,j,k}+\sin(\gamma)^2\left(\sum_{l=1}^{P}B^{(1)}{}_{i,l}u_{l,j,k}\right)u_{i,j,k}+\left(\sum_{l=1}^{P}B^{(1)}{}_{i,l}v_{l,j,k}\right)$$
$$v_{i,j,k}+\sin(\gamma)\left(\left(\sum_{l=1}^{P}B^{(1)}{}_{i,l}u_{l,j,k}\right)\left(\sum_{m=1}^{M}C^{(1)}{}_{j,m}v_{j,m,k}\right)+u_{i,j,k}\left(\sum_{m=1}^{M}\sum_{l=1}^{P}\right.\right.$$
$$C^{(1)}{}_{j,m}B^{(1)}{}_{i,l}v_{l,m,k}\Big)-\left(\sum_{l=1}^{P}B^{(1)}{}_{i,l}v_{l,j,k}\right)\Big(\sum_{m=1}^{M}C^{(1)}{}_{j,m}u_{j,m,k}\Big)-v_{i,j,k}\left(\sum_{m=1}^{M}\right.$$
$$\left.\left.\sum_{l=1}^{P}C^{(1)}{}_{j,m}B^{(1)}{}_{i,l}u_{l,m,k}\right)\right)+\cos(\gamma)\left(\left(\sum_{l=1}^{P}B^{(1)}{}_{i,l}w_{l,j,k}\right)\left(\sum_{m=1}^{M}C^{(1)}{}_{j,m}v_{j,m,k}\right.\right.$$
$$\left.\left.\Big)+w_{i,j,k}\left(\sum_{m=1}^{M}\sum_{l=1}^{P}C^{(1)}{}_{j,m}B^{(1)}{}_{i,l}v_{l,m,k}\right)-\left(\sum_{l=1}^{P}B^{(2)}{}_{i,l}w_{l,j,k}\right)v_{i,j,k}-v_{i,j,k}\right.\right.$$
$$\left.\left.\left(\sum_{m=1}^{M}\sum_{l=1}^{P}C^{(1)}{}_{j,m}B^{(1)}{}_{i,l}w_{l,m,k}\right)\right)-\sin(\gamma)Z^2\left(\left(\sum_{m=1}^{M}C^{(1)}{}_{j,m}v_{j,m,k}\right)+w_{i,j,k}\right.\right.$$
$$\left.\left.\cos(\gamma)+u_{i,j,k}\sin(\gamma)\right)+Z\left(\left(\sum_{m=1}^{M}\sum_{l=1}^{P}C^{(1)}{}_{j,m}B^{(1)}{}_{i,l}v_{l,m,k}\right)+\left(\sum_{l=1}^{P}B^{(1)}{}_{i,l}\right.\right.$$
$$\left.\left.w_{l,j,k}\right)\cos(\gamma)+\left(\sum_{l=1}^{P}B^{(1)}{}_{i,l}u_{l,j,k}\right)\sin(\gamma)\right)+\sum_{n=1}^{N}\sum_{l=1}^{P}A^{(1)}{}_{k,n}B^{(1)}{}_{i,l}w_{l,j,n}+$$
$$\left.\left.\left(\sum_{n=1}^{N}A^{(1)}{}_{k,n}w_{i,j,n}\right)\left(\sum_{n=1}^{N}\sum_{l=1}^{P}A^{(1)}{}_{k,n}B^{(1)}{}_{i,l}w_{l,j,n}\right)\right)\right)+\frac{E_0\frac{n}{h_{sh}}(1+\frac{\zeta_i}{h_{sh}})^{n-1}}{2(1+\upsilon)}$$
$$\left(\left(\sum_{n=1}^{N}A^{(1)}{}_{k,n}u_{i,j,n}\right)+\left(\sum_{l=1}^{P}B^{(1)}{}_{i,l}w_{l,j,k}\right)+\left(\sum_{l=1}^{P}B^{(1)}{}_{i,l}w_{l,j,k}\right)\right.$$
$$\left.\sum_{n=1}^{N}A^{(1)}{}_{k,n}w_{i,j,n}\right)\Big)+\frac{E_9(1+\frac{\zeta_i}{h_{sh}})^n}{2(1+\upsilon)}\left(\left(\sum_{n=1}^{N}A^{(2)}{}_{k,n}u_{i,j,n}\right)+\left(\sum_{n=1}^{N}\right.\right.$$
$$\left.\left.\sum_{l=1}^{P}A^{(1)}{}_{k,n}B^{(1)}{}_{i,l}w_{l,j,n}\right)+\left(\sum_{n=1}^{N}\sum_{l=1}^{P}A^{(1)}{}_{k,n}B^{(1)}{}_{i,l}w_{l,j,n}\right)\left(\sum_{n=1}^{N}\right.\right.$$
$$\left.\left.A^{(1)}{}_{k,n}w_{i,j,n}\right)+\left(\sum_{l=1}^{P}B^{(1)}{}_{i,l}w_{l,j,k}\right)\left(\sum_{n=1}^{N}A^{(2)}{}_{k,n}w_{i,j,n}\right)\right)+Z$$
$$\left(\frac{E_9(1+\frac{\zeta_i}{h_{sh}})^n(1-2\upsilon)}{(1+\upsilon)(1-2\upsilon)}\left(\sum_{l=1}^{P}B^{(1)}{}_{i,l}u_{l,j,k}+0.5\left(\sum_{l=1}^{P}B^{(1)}{}_{i,l}w_{l,j,k}\right)^2\right.\right.$$
$$-\left(Z^2\left(\cos(\gamma)\sin(\gamma)u_{i,j,k}w_{i,j,k}+0.5\left(\cos(\gamma)^2w_{i,j,k}{}^2+\sin(\gamma)^2\right.\right.\right.$$
$$\left.\left.\left.u_{i,j,k}{}^2+v_{i,j,k}{}^2\right)+\sin(\gamma)\left(u_{i,j,k}\left(\sum_{m=1}^{M}C^{(1)}{}_{j,m}v_{j,m,k}\right)-v_{i,j,k}\left(\sum_{m=1}^{M}\right.\right.\right.$$
$$\left.\left.\left.C^{(1)}{}_{j,m}u_{j,m,k}\right)\right)+\cos(\gamma)\left(w_{i,j,k}\left(\sum_{m=1}^{M}C^{(1)}{}_{j,m}v_{j,m,k}\right)-v_{i,j,k}\right.\right.$$
$$\left.\left.\left.\left(\sum_{m=1}^{M}C^{(1)}{}_{j,m}w_{j,m,k}\right)\right)\right)+Z\left(\left(\sum_{m=1}^{M}C^{(1)}{}_{j,m}v_{j,m,k}\right)+w_{i,j,k}\cos(\gamma)+\right.\right.$$

$$u_{i,j,k}\sin(\gamma)\Big)\Big)\sin(\gamma)+\frac{E_9(1+\frac{\zeta_i}{h_{sh}})^n}{2(1+\upsilon)}\Big(Z\Big(\Big(\sum_{m=1}^{M}C^{(1)}{}_{j,m}u_{j,m,k}\Big)-\sin(\gamma)\Big(\sum_{m=1}^{M}C^{(1)}{}_{j,m}v_{j,m,k}\Big)+\Big(\sum_{l=1}^{P}B^{(1)}{}_{i,l}w_{l,j,k}\Big)\Big(\sum_{m=1}^{M}C^{(2)}{}_{j,m}w_{j,m,k}\Big)+\Big(\sum_{m=1}^{M}\sum_{l=1}^{P}C^{(1)}{}_{j,m}B^{(1)}{}_{i,l}w_{l,m,k}\Big)\Big(\sum_{m=1}^{M}C^{(1)}{}_{j,m}w_{j,m,k}\Big)+\Big(\sum_{m=1}^{M}\sum_{l=1}^{P}C^{(1)}{}_{j,m}B^{(1)}{}_{i,l}v_{l,m,k}\Big)\Big(w_{i,j,k}\cos(\gamma)+u_{i,j,k}\sin(\gamma)\Big)+\Big(\sum_{l=1}^{P}B^{(1)}{}_{i,l}v_{l,j,k}\Big)\Big(\Big(\sum_{m=1}^{M}C^{(1)}{}_{j,m}w_{j,m,k}\Big)\cos(\gamma)+\Big(\sum_{m=1}^{M}C^{(1)}{}_{j,m}u_{j,m,k}\Big)\sin(\gamma)\Big)-\sin(\gamma)\Big(\sum_{m=1}^{M}\sum_{l=1}^{P}C^{(1)}{}_{j,m}B^{(1)}{}_{i,l}u_{l,m,k}\Big)v_{i,j,k}-\sin(\gamma)\Big(\sum_{l=1}^{P}B^{(1)}{}_{i,l}u_{l,j,k}\Big)\Big(\sum_{m=1}^{M}C^{(1)}{}_{j,m}v_{j,m,k}\Big)-\cos(\gamma)\Big(\sum_{m=1}^{M}\sum_{l=1}^{P}C^{(1)}{}_{j,m}B^{(1)}{}_{i,l}w_{l,m,k}\Big)v_{i,j,k}-\cos(\gamma)\Big(\sum_{l=1}^{P}B^{(1)}{}_{i,l}w_{l,j,k}\Big)\Big(\sum_{m=1}^{M}C^{(1)}{}_{j,m}v_{j,m,k}\Big)\Big)+\Big(\sum_{m=1}^{M}\sum_{l=1}^{P}C^{(1)}{}_{j,m}B^{(1)}{}_{i,l}v_{l,m,k}\Big)+\Big(\sum_{n=1}^{N}A^{(1)}{}_{k,n}u_{i,j,n}\Big)\Big(\sum_{l=1}^{P}B^{(1)}{}_{i,l}w_{l,j,k}\Big)+\Big(\sum_{l=1}^{P}B^{(1)}{}_{i,l}w_{l,j,k}\Big)\Big(\sum_{n=1}^{N}A^{(1)}{}_{k,n}w_{i,j,n}\Big)\Big)\cos(\gamma)\Big)=0 \qquad A_2$$

The DQ form of the equilibrium equation in circumferential direction:

$$Z\Bigg(\frac{E_0(1+\frac{\zeta_i}{h_{sh}})^n}{(1+\upsilon)(1-2\upsilon)}\Bigg((1-\upsilon)\Bigg(Z^2\Bigg(\cos(\gamma)\sin(\gamma)\Bigg(u_{i,j,k}\Big(\sum_{m=1}^{M}C^{(1)}{}_{j,m}w_{j,m,k}\Big)+w_{i,j,k}\Big(\sum_{m=1}^{M}C^{(1)}{}_{j,m}u_{j,m,k}\Big)\Bigg)+\cos(\gamma)^2w_{i,j,k}\Big(\sum_{m=1}^{M}C^{(1)}{}_{j,m}w_{j,m,k}\Big)+\sin(\gamma)^2u_{i,j,k}\Big(\sum_{m=1}^{M}C^{(1)}{}_{j,m}u_{j,m,k}\Big)+v_{i,j,k}\Big(\sum_{m=1}^{M}C^{(1)}{}_{j,m}v_{j,m,k}\Big)+\sin(\gamma)\Big(u_{i,j,k}\Big(\sum_{m=1}^{M}C^{(2)}{}_{j,m}v_{j,m,k}\Big)-v_{i,j,k}\Big(\sum_{m=1}^{M}C^{(2)}{}_{j,m}u_{j,m,k}\Big)\Big)+\cos(\gamma)\Big(w_{i,j,k}\Big(\sum_{m=1}^{M}C^{(2)}{}_{j,m}v_{j,m,k}\Big)-w_{i,j,k}\Big(\sum_{m=1}^{M}C^{(2)}{}_{j,m}u_{j,m,k}\Big)\Big)\Big)+Z\Big(\Big(\sum_{m=1}^{M}C^{(2)}{}_{j,m}v_{j,m,k}\Big)+\cos(\gamma)\Big(\sum_{m=1}^{M}C^{(1)}{}_{j,m}w_{j,m,k}\Big)+\sin(\gamma)\Big(\sum_{m=1}^{M}C^{(1)}{}_{j,m}u_{j,m,k}\Big)\Big)\Big)+\upsilon\Big(\sum_{m=1}^{M}\sum_{l=1}^{P}C^{(1)}{}_{j,m}B^{(1)}{}_{i,l}u_{l,m,k}+\sum_{n=1}^{N}\sum_{m=1}^{M}A^{(1)}{}_{k,n}C^{(1)}{}_{j,m}w_{i,m,n}+\Big(\sum_{l=1}^{P}B^{(1)}{}_{i,l}w_{l,j,k}\Big)\Big(\sum_{m=1}^{M}\sum_{l=1}^{P}C^{(1)}{}_{j,m}B^{(1)}{}_{i,l}w_{l,m,k}\Big)+\Big(\sum_{n=1}^{N}A^{(1)}{}_{k,n}w_{i,j,n}\Big)\Big(\sum_{n=1}^{N}\sum_{m=1}^{M}A^{(1)}{}_{k,n}C^{(1)}{}_{j,m}w_{i,m,n}\Big)\Big)\Big)+\frac{E_0(1+\frac{\zeta_i}{h_{sh}})^n}{(1+\upsilon)}\Big(Z\Big(\Big(\sum_{m=1}^{M}C^{(1)}{}_{j,m}u_{j,m,k}\Big)-\sin(\gamma)v_{i,j,k}+\Big(\sum_{l=1}^{P}B^{(1)}{}_{i,l}w_{l,j,k}\Big)\Big(\sum_{m=1}^{M}C^{(1)}{}_{j,m}w_{j,m,k}\Big)+\Big(\sum_{l=1}^{P}B^{(1)}{}_{i,l}v_{l,j,k}\Big)\Big(\cos(\gamma)w_{i,j,k}+\sin(\gamma)u_{i,j,k}\Big)-\sin(\gamma)v_{i,j,k}\Big(\sum_{l=1}^{P}B^{(1)}{}_{i,l}u_{l,j,k}\Big)-\cos(\gamma)v_{i,j,k}\Big(\sum_{l=1}^{P}B^{(1)}{}_{i,l}w_{l,j,k}\Big)\Big)\Big)\Big)\sin(\gamma)+\Bigg(\frac{n}{h_{sh}}\frac{E_0(1+\frac{\zeta_i}{h_{sh}})^{n-1}}{2(1+\upsilon)}+2ZE_0(1+\frac{\zeta_i}{h_{sh}})^n$$

$$\cos(\gamma)\Big)\Big(Z\Big(\big(\cos(\gamma)w_{i,j,k}+\sin(\gamma)u_{i,j,k}\big)\Big(\sum_{n=1}^{N}A^{(1)}{}_{k,n}v_{i,j,n}\Big)+\Big(\Big(\sum_{m=1}^{M}C^{(1)}{}_{j,m}w_{j,m,k}\Big)-\cos(\gamma)v_{i,j,k}\Big)\Big(\sum_{n=1}^{N}A^{(1)}{}_{k,n}w_{i,j,n}\Big)-\cos(\gamma)v_{i,j,k}-\sin(\gamma)v_{i,j,k}\Big(\sum_{n=1}^{N}A^{(1)}{}_{k,n}u_{i,j,n}\Big)+\Big(\sum_{m=1}^{M}C^{(1)}{}_{j,m}w_{j,m,k}\Big)\Big)+\Big(\sum_{n=1}^{N}A^{(1)}{}_{k,n}v_{i,j,n}\Big)\Big)+\frac{E_0(1+\frac{\zeta_i}{h_{sh}})^n}{2(1+\upsilon)}\Big(Z\big(\cos(\gamma)w_{i,j,k}+\sin(\gamma)u_{i,j,k}\big)\Big(\sum_{n=1}^{N}A^{(2)}{}_{k,n}v_{i,j,n}\Big)+\Big(\cos(\gamma)\Big(\sum_{n=1}^{N}A^{(1)}{}_{k,n}w_{i,j,n}\Big)+\sin(\gamma)\Big(\sum_{n=1}^{N}A^{(1)}{}_{k,n}u_{i,j,n}\Big)\Big)\Big(\sum_{n=1}^{N}A^{(1)}{}_{k,n}v_{i,j,n}\Big)+\Big(\Big(\sum_{m=1}^{M}C^{(1)}{}_{j,m}w_{j,m,k}\Big)-\cos(\gamma)v_{i,j,k}\Big)\Big(\sum_{n=1}^{N}A^{(2)}{}_{k,n}w_{i,j,n}\Big)+\Big(\Big(\sum_{n=1}^{N}\sum_{m=1}^{M}A^{(1)}{}_{k,n}C^{(1)}{}_{j,m}w_{i,m,n}\Big)-\cos(\gamma)\Big(\sum_{n=1}^{N}A^{(1)}{}_{k,n}v_{i,j,n}\Big)\Big)\Big(\sum_{n=1}^{N}A^{(1)}{}_{k,n}w_{i,j,n}\Big)-\cos(\gamma)\Big(\sum_{n=1}^{N}A^{(1)}{}_{k,n}v_{i,j,n}\Big)-\sin(\gamma)\Big(\sum_{n=1}^{N}A^{(1)}{}_{k,n}v_{i,j,n}\Big)\Big(\sum_{n=1}^{N}A^{(1)}{}_{k,n}u_{i,j,n}\Big)-\sin(\gamma)v_{i,j,k}\Big(\sum_{n=1}^{N}A^{(2)}{}_{k,n}u_{i,j,n}\Big)+\Big(\sum_{n=1}^{N}\sum_{m=1}^{M}A^{(1)}{}_{k,n}C^{(1)}{}_{j,m}w_{i,m,n}\Big)\Big)+\Big(\sum_{n=1}^{N}A^{(2)}{}_{k,n}v_{i,j,n}\Big)-\cos(\gamma)Z^2\Big(\big(\cos(\gamma)w_{i,j,k}+\sin(\gamma)u_{i,j,k}\big)\Big(\sum_{n=1}^{N}A^{(1)}{}_{k,n}v_{i,j,n}\Big)+\Big(\Big(\sum_{m=1}^{M}C^{(1)}{}_{j,m}w_{j,m,k}\Big)-\cos(\gamma)v_{i,j,k}\Big)\Big(\sum_{n=1}^{N}A^{(1)}{}_{k,n}w_{i,j,n}\Big)-\cos(\gamma)v_{i,j,k}-\sin(\gamma)v_{i,j,k}\Big(\sum_{n=1}^{N}A^{(1)}{}_{k,n}+u_{i,j,n}\Big)+\Big(\sum_{m=1}^{M}C^{(1)}{}_{j,m}w_{j,m,k}\Big)\Big)\frac{E_0(1+\frac{\zeta_i}{h_{sh}})^n}{2(1+\upsilon)}\Big(Z\Big(\Big(\cos(\gamma)\Big(\sum_{l=1}^{P}B^{(1)}{}_{i,l}w_{l,j,k}\Big)+\sin(\gamma)\Big(\sum_{l=1}^{P}B^{(1)}{}_{i,l}u_{l,j,k}\Big)\Big)\Big(\sum_{n=1}^{N}A^{(1)}{}_{k,n}v_{i,j,n}\Big)+\big(\cos(\gamma)w_{i,j,k}+\sin(\gamma)u_{i,j,k}\big)\Big(\sum_{n=1}^{N}\sum_{l=1}^{P}A^{(1)}{}_{k,n}B^{(1)}{}_{i,l}v_{l,j,n}\Big)+\Big(\Big(\sum_{m=1}^{M}\sum_{l=1}^{P}C^{(1)}{}_{j,m}B^{(1)}{}_{i,l}w_{l,m,k}\Big)-\cos(\gamma)\Big(\sum_{l=1}^{P}B^{(1)}{}_{i,l}u_{l,j,k}\Big)\Big)\Big(\sum_{n=1}^{N}A^{(1)}{}_{k,n}w_{i,j,n}\Big)+\Big(\Big(\sum_{m=1}^{M}C^{(1)}{}_{j,m}w_{j,m,k}\Big)-\cos(\gamma)v_{i,j,k}\Big)\Big(\sum_{n=1}^{N}\sum_{l=1}^{P}A^{(1)}{}_{k,n}B^{(1)}{}_{i,l}w_{l,j,n}\Big)-\cos(\gamma)\Big(\sum_{l=1}^{P}B^{(1)}{}_{i,l}v_{l,j,k}\Big)-\sin(\gamma)\Big(\sum_{l=1}^{P}B^{(1)}{}_{i,l}v_{l,j,k}\Big)\Big(\sum_{n=1}^{N}A^{(1)}{}_{k,n}u_{i,j,n}\Big)-\sin(\gamma)v_{i,j,k}\Big(\sum_{n=1}^{N}\sum_{l=1}^{P}A^{(1)}{}_{k,n}B^{(1)}{}_{i,l}u_{l,j,n}\Big)+\Big(\sum_{m=1}^{M}\sum_{l=1}^{P}C^{(1)}{}_{j,m}B^{(1)}{}_{i,l}w_{l,m,k}\Big)\Big)+\Big(\sum_{l=1}^{P}B^{(2)}{}_{i,l}v_{l,j,k}\Big)\Big)+\frac{E_0(1+\frac{\zeta_i}{h_{sh}})^n}{2(1+\upsilon)}\Big(\Big(\sum_{n=1}^{N}A^{(1)}{}_{k,n}u_{i,j,n}\Big)+\Big(\sum_{l=1}^{P}B^{(1)}{}_{i,l}w_{l,j,k}\Big)+\Big(\sum_{l=1}^{P}B^{(1)}{}_{i,l}w_{l,j,k}\Big)\Big(\sum_{n=1}^{N}A^{(1)}{}_{k,n}w_{i,j,n}\Big)\Big)\sin(\gamma)+\frac{E_0(1+\frac{\zeta_i}{h_{sh}})^n(2\upsilon-1)}{(1+\upsilon)(1-2\upsilon)}$$

$$\left(Z^2\left(\cos(\gamma)\sin(\gamma)u_{i,j,k}w_{i,j,k}+0.5\sin(\gamma)u_{l,j,k}\right)v_{i,j,k}-\cos(\gamma)\left(\sum_{l=1}^{P}\right.\right.$$
$$B^{(1)}{}_{i,l}w_{l,j,k}\Big)v_{i,j,k}\Big)+\left(\sum_{l=1}^{P}B^{(1)}{}_{i,l}v_{l,j,k}\right)\Big)+\frac{E_0(1+\frac{\zeta_i}{h_{sh}})^n}{2(1+\upsilon)}Z\Big(\Big(\sum_{m=1}^{M}\sum_{l=1}^{P}C^{(1)}{}_{j,m}$$
$$B^{(1)}{}_{i,l}u_{l,m,k}\Big)-\Big(\sum_{l=1}^{P}B^{(1)}{}_{i,l}v_{l,j,k}\Big)+\Big(\sum_{l=1}^{P}B^{(2)}{}_{i,l}w_{l,j,k}\Big)\Big(\sum_{m=1}^{M}C^{(1)}{}_{j,m}w_{j,m,k}\Big)+$$
$$\Big(\sum_{l=1}^{P}B^{(1)}{}_{i,l}w_{l,j,k}\Big)\Big(\sum_{m=1}^{M}\sum_{l=1}^{P}C^{(1)}{}_{j,m}B^{(1)}{}_{i,l}w_{l,m,k}\Big)+\Big(\sum_{l=1}^{P}B^{(2)}{}_{i,l}v_{l,j,k}\Big)\Big(\cos(\gamma)$$
$$w_{i,j,k}+\sin(\gamma)u_{i,j,k}\Big)-\sin(\gamma)\Big(\sum_{l=1}^{P}B^{(2)}{}_{i,l}u_{l,j,k}\Big)v_{i,j,k}-\cos(\gamma)\Big(\sum_{l=1}^{P}B^{(2)}{}_{i,l}$$
$$w_{l,j,k}\Big)v_{i,j,k}\Big)+\Big(\sum_{l=1}^{P}B^{(2)}{}_{i,l}v_{l,j,k}\Big)\Big)=0 \qquad A_3$$

The DQ form of the equilibrium equation in ζ direction.

$$\frac{E_0(1+\frac{\zeta_i}{h_{sh}})^n}{2(1+\upsilon)}\Big(\Big(\sum_{n=1}^{N}\sum_{l=1}^{P}A^{(1)}{}_{k,n}B^{(1)}{}_{i,l}u_{l,j,n}\Big)+\Big(\sum_{l=1}^{P}B^{(2)}{}_{i,l}w_{l,j,k}\Big)+\Big(\sum_{l=1}^{P}B^{(2)}{}_{i,l}$$
$$w_{l,j,k}\Big)\Big(\sum_{n=1}^{N}A^{(1)}{}_{k,n}w_{i,j,n}\Big)+\Big(\sum_{l=1}^{P}B^{(1)}{}_{i,l}w_{l,j,k}\Big)\Big(\sum_{n=1}^{N}\sum_{l=1}^{P}A^{(1)}{}_{k,n}B^{(1)}{}_{i,l}w_{l,j,n}\Big)\Big)$$
$$+\frac{E_0\frac{n}{h_{sh}}(1+\frac{\zeta_i}{h_{sh}})^{n-1}}{(1+\upsilon)(1-2\upsilon)}\Big(\upsilon\Big(\sum_{l=1}^{P}B^{(1)}{}_{i,l}u_{l,j,k}+0.5\Big(\sum_{l=1}^{P}B^{(1)}{}_{i,l}w_{l,j,k}\Big)^2+Z^2$$
$$\left(\cos(\gamma)\sin(\gamma)u_{i,j,k}w_{i,j,k}+0.5\left(\cos(\gamma)^2{w_{i,j,k}}^2+\sin(\gamma)^2{u_{i,j,k}}^2+\right.\right.$$
$${v_{i,j,k}}^2\Big)+\sin(\gamma)\Big(u_{i,j,k}\Big(\sum_{m=1}^{M}C^{(1)}{}_{j,m}v_{j,m,k}\Big)-v_{i,j,k}\Big(\sum_{m=1}^{M}C^{(1)}{}_{j,m}u_{j,m,k}\Big)\Big)+$$
$$\cos(\gamma)\Big(w_{i,j,k}\Big(\sum_{m=1}^{M}C^{(1)}{}_{j,m}v_{j,m,k}\Big)-v_{i,j,k}\Big(\sum_{m=1}^{M}C^{(1)}{}_{j,m}w_{j,m,k}\Big)\Big)\Big)+Z\Big($$
$$\Big(\sum_{m=1}^{M}C^{(1)}{}_{j,m}v_{j,m,k}\Big)+w_{i,j,k}\cos(\gamma)+u_{i,j,k}\sin(\gamma)\Big)\Big)\Big)+(1-\upsilon)\Big(\sum_{n=1}^{N}$$
$$A^{(1)}{}_{k,n}w_{i,j,n}+0.5\Big(\sum_{n=1}^{N}A^{(1)}{}_{k,n}w_{i,j,n}\Big)^2\Big)\Big)+\frac{E_0(1+\frac{\zeta_i}{h_{sh}})^n}{(1+\upsilon)(1-2\upsilon)}\Big(\upsilon\Big(\Big(\sum_{n=1}^{N}$$
$$\sum_{l=1}^{P}A^{(1)}{}_{k,n}B^{(1)}{}_{i,l}u_{l,j,n}+\Big(\sum_{l=1}^{P}B^{(1)}{}_{i,l}w_{l,j,k}\Big)\Big(\sum_{n=1}^{N}\sum_{l=1}^{P}A^{(1)}{}_{k,n}B^{(1)}{}_{i,l}w_{l,j,n}\Big)+ \qquad A_4$$
$$Z^2\Big(\cos(\gamma)\sin(\gamma)\Big(\Big(\sum_{n=1}^{N}A^{(1)}{}_{k,n}u_{i,j,n}\Big)w_{i,j,k}+\Big(\sum_{n=1}^{N}A^{(1)}{}_{k,n}w_{i,j,n}\Big)u_{i,j,k}$$
$$\Big)+\cos(\gamma)^2\Big(\sum_{n=1}^{N}A^{(1)}{}_{k,n}w_{i,j,n}\Big)w_{i,j,k}+\sin(\gamma)^2\Big(\sum_{n=1}^{N}A^{(1)}{}_{k,n}u_{i,j,n}\Big)u_{i,j,k}$$
$$+\Big(\sum_{n=1}^{N}A^{(1)}{}_{k,n}v_{i,j,n}\Big)v_{i,j,k}+\sin(\gamma)\Big(\Big(\sum_{n=1}^{N}A^{(1)}{}_{k,n}u_{i,j,n}\Big)\Big(\sum_{m=1}^{M}C^{(1)}{}_{j,m}v_{j,m,k}\Big)$$
$$+u_{i,j,k}\Big(\sum_{n=1}^{N}\sum_{m=1}^{M}A^{(1)}{}_{k,n}C^{(1)}{}_{j,m}v_{i,m,n}\Big)-\Big(\sum_{n=1}^{N}A^{(1)}{}_{k,n}v_{i,j,n}\Big)\Big(\sum_{m=1}^{M}C^{(1)}{}_{j,m}u_{j,m,k}\Big)$$
$$-v_{i,j,k}\Big(\sum_{n=1}^{N}\sum_{m=1}^{M}A^{(1)}{}_{k,n}C^{(1)}{}_{j,m}u_{i,m,n}\Big)\Big)+\cos(\gamma)\Big(\Big(\sum_{n=1}^{N}A^{(1)}{}_{k,n}w_{i,j,n}$$
$$\Big(\sum_{m=1}^{M}C^{(1)}{}_{j,m}v_{j,m,k}\Big)+\Big(\sum_{n=1}^{N}\sum_{m=1}^{M}A^{(1)}{}_{k,n}C^{(1)}{}_{j,m}v_{i,m,n}\Big)w_{i,j,k}-\Big(\sum_{n=1}^{N}A^{(1)}{}_{k,n}v_{i,j,n}\Big)$$
$$\Big(\sum_{m=1}^{M}C^{(1)}{}_{j,m}w_{j,m,k}\Big)-\Big(\sum_{n=1}^{N}\sum_{m=1}^{M}A^{(1)}{}_{k,n}C^{(1)}{}_{j,m}w_{i,m,n}\Big)v_{i,j,k}\Big)\Big)+Z\Big(\Big(\sum_{n=1}^{N}\sum_{m=1}^{M}$$
$$A^{(1)}{}_{k,n}C^{(1)}{}_{j,m}v_{i,m,n}\Big)+\Big(\sum_{n=1}^{N}A^{(1)}{}_{k,n}w_{i,j,n}\Big)\cos(\gamma)+\Big(\sum_{n=1}^{N}A^{(1)}{}_{k,n}u_{i,j,n}\Big)\sin(\gamma)$$
$$\Big)\Big)-2\cos(\gamma)Z^3\Big(\cos(\gamma)\sin(\gamma)u_{i,j,k}w_{i,j,k}+0.5\Big(\cos(\gamma)^2{w_{i,j,k}}^2+$$
$$\sin(\gamma)^2\Big(\sum_{n=1}^{N}\sum_{m=1}^{M}A^{(1)}{}_{k,n}C^{(1)}{}_{j,m}v_{i,m,n}\Big)\Big)+\sin(\gamma)\Big(u_{i,j,k}\Big(\sum_{m=1}^{M}C^{(1)}{}_{j,m}v_{j,m,k}\Big)$$
$$-v_{i,j,k}\Big(\sum_{m=1}^{M}C^{(1)}{}_{j,m}u_{j,m,k}\Big)\Big)+\cos(\gamma)\Big(w_{i,j,k}\Big(\sum_{m=1}^{M}C^{(1)}{}_{j,m}v_{j,m,k}\Big)-v_{i,j,k}$$
$$\Big(\sum_{m=1}^{M}C^{(1)}{}_{j,m}w_{j,m,k}\Big)\Big)\Big)-\cos(\gamma)Z^2\Big(\Big(\sum_{m=1}^{M}C^{(1)}{}_{j,m}v_{j,m,k}\Big)+w_{i,j,k}\cos(\gamma)$$
$$+u_{i,j,k}\sin(\gamma)\Big)\Big)\Big)+Z\Bigg(\frac{E_0(1+\frac{\zeta_i}{h_{sh}})^n}{2(1+\upsilon)}\Big(Z\Big(\Big(\cos(\gamma)\Big(\sum_{m=1}^{M}C^{(1)}{}_{j,m}w_{j,m,k}\Big)+$$
$$\sin(\gamma)\Big(\sum_{m=1}^{M}C^{(1)}{}_{j,m}u_{j,m,k}\Big)\Big)\Big(\sum_{n=1}^{N}A^{(1)}{}_{k,n}v_{i,j,n}\Big)+\Big(\cos(\gamma)w_{i,j,k}+\sin(\gamma)$$
$$u_{i,j,k}\Big)\Big(\sum_{n=1}^{N}\sum_{m=1}^{M}A^{(1)}{}_{k,n}C^{(1)}{}_{j,m}v_{i,m,n}\Big)+\Big(\Big(\sum_{m=1}^{M}C^{(2)}{}_{j,m}w_{j,m,k}\Big)-\cos(\gamma)\Big($$
$$\sum_{m=1}^{M}C^{(1)}{}_{j,m}v_{j,m,k}\Big)\Big)\Big(\sum_{n=1}^{N}A^{(1)}{}_{k,n}w_{i,j,n}\Big)+\Big(\Big(\sum_{m=1}^{M}C^{(1)}{}_{j,m}w_{j,m,k}\Big)-\cos(\gamma)v_{i,j,k}\Big)$$
$$\Big(\sum_{n=1}^{N}\sum_{m=1}^{M}A^{(1)}{}_{k,n}C^{(1)}{}_{j,m}w_{i,m,n}\Big)-\cos(\gamma)\Big(\sum_{m=1}^{M}C^{(1)}{}_{j,m}v_{j,m,k}\Big)-\sin(\gamma)\Big(\sum_{m=1}^{M}$$
$$C^{(1)}{}_{j,m}v_{j,m,k}\Big)\Big(\sum_{n=1}^{N}A^{(1)}{}_{k,n}u_{i,j,n}\Big)-\sin(\gamma)v_{i,j,k}\Big(\sum_{n=1}^{N}\sum_{m=1}^{M}A^{(1)}{}_{k,n}C^{(1)}{}_{j,m}u_{i,m,n}\Big)$$
$$+\Big(\sum_{m=1}^{M}C^{(2)}{}_{j,m}w_{j,m,k}\Big)\Big)+\Big(\sum_{n=1}^{N}\sum_{m=1}^{M}A^{(1)}{}_{k,n}C^{(1)}{}_{j,m}v_{i,m,n}\Big)\Big)+\frac{E_0(1+\frac{\zeta_i}{h_{sh}})^n}{2(1+\upsilon)}\Big($$
$$\Big(\sum_{n=1}^{N}A^{(1)}{}_{k,n}u_{i,j,n}\Big)+\Big(\sum_{l=1}^{P}B^{(1)}{}_{i,l}w_{l,j,k}\Big)+\Big(\sum_{l=1}^{P}B^{(1)}{}_{i,l}w_{l,j,k}\Big)\Big(\sum_{n=1}^{N}A^{(1)}{}_{k,n}w_{i,j,n}\Big)\Big)$$
$$\sin(\gamma)+\frac{E_0(1+\frac{\zeta_i}{h_{sh}})^n(2\upsilon-1)}{(1+\upsilon)(1-2\upsilon)}\Big(Z^2\Big(\cos(\gamma)\sin(\gamma)u_{i,j,k}w_{i,j,k}+0.5\Big($$
$$\cos(\gamma)^2{w_{i,j,k}}^2+\sin(\gamma)^2{u_{i,j,k}}^2+{v_{i,j,k}}^2\Big)+\sin(\gamma)\Big(u_{i,j,k}\Big(\sum_{m=1}^{M}C^{(1)}{}_{j,m}v_{j,m,k}\Big)$$
$$-v_{i,j,k}\Big(\sum_{m=1}^{M}C^{(1)}{}_{j,m}u_{j,m,k}\Big)\Big)+\cos(\gamma)\Big(w_{i,j,k}\Big(\sum_{m=1}^{M}C^{(1)}{}_{j,m}v_{j,m,k}\Big)-v_{i,j,k}\Big(\sum_{m=1}^{M}$$
$$C^{(1)}{}_{j,m}w_{j,m,k}\Big)\Big)\Big)+Z\Big(\Big(\sum_{m=1}^{M}C^{(1)}{}_{j,m}v_{j,m,k}\Big)+w_{i,j,k}\cos(\gamma)+u_{i,j,k}\sin(\gamma)\Big)-$$
$$\Big(\sum_{n=1}^{N}A^{(1)}{}_{k,n}w_{i,j,n}+0.5\Big(\sum_{n=1}^{N}A^{(1)}{}_{k,n}w_{i,j,n}\Big)^2\Big)\Big)\cos(\gamma)\Big)=0$$

The DQ form of boundary conditions.

$$\sigma_{\zeta\zeta}=\frac{E_0(1+\frac{\zeta_i}{h_{sh}})^n(\upsilon)}{(1+\upsilon)(1-2\upsilon)}\left(\left(\sum_{m=1}^{M}C^{(1)}{}_{j,m}u_{j,m,k}\right)+0.5\left(\sum_{m=1}^{M}C^{(1)}{}_{j,m}w_{j,m,k}\right)^2\right.$$

$$\left.-\alpha_0(1+\frac{\zeta_i}{h_{sh}})^nT_{i,j,k}\right)+\frac{E_0(1+\frac{\zeta_i}{h_{sh}})^n(\upsilon)}{(1+\upsilon)(1-2\upsilon)}\left(Z^2\left(\cos(\gamma)\sin(\gamma)u_{i,j,k}w_{i,j,k}\right.\right.$$

$$+0.5\left(\cos(\gamma)^2w_{i,j,k}{}^2+\sin(\gamma)^2u_{i,j,k}{}^2+v_{i,j,k}{}^2\right)+\sin(\gamma)\left(u_{i,j,k}\left(\sum_{m=1}^{M}\right.\right.$$

$$C^{(1)}{}_{j,m}v_{j,m,k}\Big)-v_{i,j,k}\left(\sum_{m=1}^{M}C^{(1)}{}_{j,m}u_{j,m,k}\right)\Big)+\cos(\gamma)\left(w_{i,j,k}\left(\sum_{m=1}^{M}C^{(1)}{}_{j,m}\right.\right.$$

$$\left.\left.v_{j,m,k}\Big)-v_{i,j,k}\left(\sum_{m=1}^{M}C^{(1)}{}_{j,m}w_{j,m,k}\right)\right)\right)+Z\left(\left(\sum_{m=1}^{M}C^{(1)}{}_{j,m}v_{j,m,k}\right)+w_{i,j,k}\cos(\gamma)\right.$$

$$\left.+u_{i,j,k}\sin(\gamma)\right)\Big)-\alpha_0(1+\frac{\zeta_i}{h_{sh}})^nT_{i,j,k}\Big)+\frac{E_0(1+\frac{\zeta_i}{h_{sh}})^n(1-\upsilon)}{(1+\upsilon)(1-2\upsilon)}\left(\left(\sum_{n=1}^{N}A^{(1)}{}_{k,n}\right.\right.$$

$$\left.\left.w_{i,j,n}\Big)+0.5\left(\sum_{n=1}^{N}A^{(1)}{}_{k,n}w_{i,j,n}\right)^2-\alpha_0(1+\frac{\zeta_i}{h_{sh}})^nT_{i,j,k}\right)=0$$

$$\tau_{\zeta\theta}=\frac{E_0(1+\frac{\zeta_i}{h_{sh}})^n}{2(1+\upsilon)}\left(Z\left(\left(\cos(\gamma)w_{i,j,k}+\sin(\gamma)u_{i,j,k}\right)\left(\sum_{n=1}^{N}A^{(1)}{}_{k,n}v_{i,j,n}\right)\right.\right.$$

$$+\left(\left(\sum_{l=1}^{P}B^{(1)}{}_{i,l}w_{l,j,k}\right)-\cos(\gamma)v_{i,j,k}\right)\left(\sum_{n=1}^{N}A^{(1)}{}_{k,n}w_{i,j,n}\right)-\cos(\gamma)v_{i,j,k}-$$

$$\left.\left.\sin(\gamma)\left(\sum_{n=1}^{N}A^{(1)}{}_{k,n}u_{i,j,n}\right)v_{i,j,k}+\left(\sum_{l=1}^{P}B^{(1)}{}_{i,l}w_{l,j,k}\right)\right)+\left(\sum_{n=1}^{N}A^{(1)}{}_{k,n}v_{i,j,n}\right)\right)=0 \qquad A_5$$

$$\tau_{s\zeta}=\frac{E_0(1+\frac{\zeta_i}{h_{sh}})^n}{2(1+\upsilon)}\left(\left(\sum_{n=1}^{N}A^{(1)}{}_{k,n}u_{i,j,n}\right)+\left(\sum_{l=1}^{P}B^{(1)}{}_{i,l}w_{l,j,k}\right)+\left(\sum_{l=1}^{P}B^{(1)}{}_{i,l}\right.\right.$$

$$\left.\left.w_{l,j,k}\right)\left(\sum_{n=1}^{N}A^{(1)}{}_{k,n}w_{i,j,n}\right)\right)=0$$

The DQ form of heat transfer equation through the thickness:

$$\left(\frac{K_0(1+\frac{\zeta_i}{h_{sh}})^n\cos(\gamma)}{R_1+\frac{1}{Z}}\right)\left(\sum_{n=1}^{N}A^{(1)}_{i,n}T_{n,j}\right)+K_0(1+\frac{\zeta_i}{h_{sh}})^n\left(\sum_{n=1}^{N}A^{(2)}_{i,n}T_{n,j}\right)+$$

$$K_0\frac{n}{h}(1+\frac{\zeta_i}{h_{sh}})^{n-1}\left(\sum_{n=1}^{N}A^{(1)}_{i,n}T_{n,j}\right)=0 \qquad A_6$$

Three-dimensional Magneto-thermo-elastic Analysis of Functionally Graded Truncated Conical Shells

A. Mehditabar, R. Akbari Alashti, M. H. Pashaei

Mechanical Engineering Department, Babol University of Technology, Babol, Iran

P A P E R I N F O

Paper history:
Received 17 April 2013
Received in revised form 18 June 2013
Accepted 20 June 2013

Keywords:
Magneto-thermo-elastic
Functionally Graded Material
Truncated Conical Shell

چکیده

در این مقاله مسئله سه بعدی مگنتو-ترمو-الاستیک پوسته مخروطی ناقص ساخته شده از ماده مدرج تابعی تحت فشار غیر یکنواخت داخلی و در حضور میدان‌های مغناطیسی و حرارتی بررسی می‌شود. خواص مواد از قانون توانی وابسته به مختصات پوسته در راستای ضخامت پیروی می‌کنند. فرمولبندی مسئله با توسعه روابط بنیادی ترمو-الاستیسیته بر حسب سیستم مختصات مخروطی آغاز می‌شود. متعاقبا از روش کوادریچر تفاضلی برای گسسته سازی و تبدیل معادلات دیفرانسیلی منتجه به سیستم معادلات جبری استفاده می‌شود. نتایج عددی تاثیرات ناهمگنی خاصیت ماده و نیروهای حرارتی بر توزیع میدان‌های جابه‌جایی، تنش، دما و مغناطیس القایی را نشان می‌دهد. از روش اجزاء محدود جهت راستی آزمایی جوابهای حاصله از روش کوادریچر تفاضلی برای پوسته مخروطی ناقص ساخته شده از ماده مدرج تابعی استفاده شده است که انطباق خوبی را نشان می‌دهد.

doi: *10.5829/idosi.ije.2013.26.12c.05*